L.N.L. - I.N.F.N. (REP) 104 / 96

# PRELIMINARY RESULTS FROM A NEW MICROSTRUCTURE FOR GASEOUS DETECTORS

*M. Lombardi, °F.S. Lombardi

*I.N.F.N. Laboratori Nazionali di Legnaro, via Romea,4 - Legnaro Italy

°Osservatorio Astronomico S. Lucia Stroncone (Terni) Italy

***Submitted to Nuclear Instruments and Methods Section A***

A cura del servizio
Documentazione dei
L.N.L.

**I.N.F.N. Laboratori Nazionali di Legnaro Via Romea, 4 - I-35020 Legnaro, Padova, Italy**

# PRELIMINARY RESULTS FROM A NEW MICROSTRUCTURE FOR GASEOUS DETECTORS

M. LOMBARDI*
INFN, Laboratori Nazionali di Legnaro, 35020 Legnaro (Padova)-Italy

F.S. LOMBARDI
Osservatorio Astronomico S.Lucia-05039-Stroncone (Terni)-Italy

**Abstract.** A new microstructure for the detection of gas ionizing radiations has been characterized. For every detected ionizing radiation it gives two "induced" charges of the same amount, of opposite sign, with the same collection time and essentially in time coincidence, that are proportional to the primary ionization collected. A gas multiplication up to $4x10^5$ was achieved. This microstructure allows the development of a position sensitive detector with a two-dimensional read-out of the two external surfaces, which are shielded from each other by an intermediate conducting layer. The latter, when connected to a low input impedance pick-up, simultaneously reduces the problems of capacitive cross-talk and gives a trigger to "coordinate" the charges (pulses) from the external surfaces generated by each detected ionizing radiation. When connected to a low impedance input, the charges from this microstructure produce pulses particularly suitable for timing, with a risetime of few ns. Using isobutane as the gas, an energy resolution of about 8% FWHM was recorded for $\alpha$ particles of 5.5 MeV from an $^{241}$Am source. Always in isobutane gas, X rays from a $^{55}$Fe source and $\beta^-$ particles from a $^{14}$C source were also detected.

---

* Corresponding Author

## 1. Introduction

The possibility to detect α particles in open room air (even if with poor characteristics) with the Corona Spark Counters is well known. Often these are named as Chang-Rosemblum counters [1].

In order to individualize a microstructure able to detect gas ionizing radiations and suitable to develop a position sensitive detecting board with a two-dimensional readout, we were interested in determining the feasibility of detecting α particles in room air starting from a condition of stability in the anodic and cathodic channels, i.e., in the absence of corona pulses and of spurious pulses produced by secondary processes. Moreover, we wondered whether dimensions and working conditions for a microstructure could be found, that would allow the generation of charges proportional to the primary ionization collected and avoiding a Geiger type behaviour [2].

We proceeded to explore these questions on the basis of, among others, the following considerations:

1) A small anode-cathode gap [3] permits a much reduced space charge, and hence a major improvement in count rate performance.

2) The detecting surface of a two-dimensional position sensitive detector should consist of several active microstructures, independent a priori from each other. It should be then possible to read the microstructures either individually or in groups, by means, for example, of microstrips. Furthermore, for each detected ionizing radiation the microstructures would have to produce two charges, one for the X, and the other for the Y coordinate. The two charges should be essentially in time coincidence and have, if possible, the same amount (that is $Q_X = Q_Y$) and the same collection time. Clearly, these last requirements can't be met by charges induced via capacitance (capacitive coupling) on a backplane, because in this case a $Q_{back}/Q_{avalanche}$ ratio of 1/5 has been reported to occur [4] . They can be met, instead, by "conductivity" as explained below.

3) The capacitive coupling (AC) behaviour has to be avoided where possible. It is well known that a capacitive coupling in an electronic chain causes a baseline offset which depends strongly on the pulse rate. This can degrade, particularly in the presence of high random counting rate, the timing as well as the energy resolution. To avoid this degradation it is necessary to use direct connection (DC) or a baseline restorer circuit must be used.

4) A two-dimensional position sensitive detector should have an element delivering very fast pulses, one for each detected ionizing radiation, and well correlated in time with the ionizing radiation to be detected. Such pulses could be then used as a trigger"to coordinate" pairs of pulses generated by the microstructures in two-dimensional X and Y coordinates.

5) A microstrip consists simply of a flat signal conductor and a ground plane separated by a dielectric with a characteristic impedance $Z_0$ which has to be properly matched to avoid signal reflections and ringing . It is important to take this into account, particularly in the case of signals with a very fast risetime and a very short duration, when long microstrips are used or when they are arranged in a delay line [5].

6) It is necessary to assemble and give the proper dimensions to the active microstructures of the detector in such a manner that the parasitic capacitances among them, causing cross-talk, are as low as possible. The capacitive cross-talk constitutes an electrical blurring of the image, produced by the primary ionization collected, on the detecting surface while, usually, the best focusing and spatial resolution are required. The capacitive cross-talk can result also in data -acquisition errors and/or generate noise, pile-up, and so on. To minimize the capacitive cross-talk is very important in every case but becomes unavoidable in two-dimension multihit conditions. The capacitive cross-talk is minimized not only by choosing a proper geometry for the active

microstructures but also strongly, if microstrips are used, matching them on their characteristic low impedance Zo. This opportunity clearly presumes that the active microstructures, which feed the microstrips, are able to work on low impedance, that is they should have to work as generators with a rather low internal impedance.

## 2.Experimental set-up

The set-up consists of a pillory made with two pieces of 3 mm thick Plexiglas (fig.1), holding a length of tungsten wire perpendicular to the pillory plane, and forming a point above it. The wire has a $\phi$=20 μm. It is possible to slide the wire-point along the axis of the pillory.

Two copper strips, ~ 3x30 $mm^2$ and 20 μm thick, were placed on the pillory plane with their borders oblique, but symmetrical to the axis of the pillory. They form a leak variable from some tens to some hundreds μm in the middle of which it is possible to slide the wire-point.

The wire-point and the nearest borders of the strips form an electrical gap ,i.e., a **leak microstructure** (LM in the following). The entire set-up was assembled manually with the help of a microscope.

High voltage (HV) is applied to the two strips, soldered together at one end, through an RC filter and through a 100 kΩ resistor (fig.1), while the wire-point is set practically at ground potential (see figs.1 and 2).

The signals from the LM are collected by the two pick-ups of fig.2 (already used elsewhere [5]) the main role of which is to protect from the sparks the vertical amplifiers of the oscilloscope used to monitor the behaviour of the LM.

The wire-point, if used as cathode, gives Trichel's pulses [6]. For this reason the wire-points are used as anodes.

An electron, produced anywhere in the gas volume, that reaches the strong electric field between the wire-point and the strips of the LM, will drift along the field line towards the anode-wire-point where it will experience an avalanche multiplication in the gas close to the surface of the point.

## 3. The LM's behaviour in open room air

It is possible to obtain, with good stability and repeatability, the following behaviour.

For a tungsten wire-point of $\phi$=20 μm and for every value of the leak in the range of b=100 up to b=300 μm or more (**b** is the distance between the borders of the strips nearest to the wire-point) there is a well definite value of the HV between anode and cathode (which we name as **threshold voltage** Vt) that gives rise to the following circumstances, in absence of a source of α particles :

1) below Vt the anodic and cathodic channels, monitored with the oscilloscope, are completely stable (lack of any discharge and of spurious pulses) and with very low noise. The current from the HV power supply (Silena mod.7716) is under the reading sensitivity of $10^{-9}$ A.

2) at Vt random pulses of ~1 mV and of ~25 ns duration abruptly take place (**above threshold pulses**). They become more and more frequent as the HV grows above Vt giving rise to pile-up and leading the LM into acoustic sparks at a well definite value **Vs (spark voltage).** One believes that these above threshold pulses are the consequence of the ejection of electrons from the cathode by field emission (this is still under investigation). The current at Vt is about $10^{-9}$A.

Fig. 3 shows Vt and Vs as functions of b for a tungsten wire-point of $\phi$=20 μm.

The evaluation of b was done with a calibrated micrometer disc reticule inserted in the microscope. For this reason the values reported in fig.3 (and in the next figs.4 and 5) give trends, rather than being precise measurements.

It is possible to obtain the same behaviour when tungsten wire-points of $\phi$=10 or $\phi$=50 μm are used, within the b range and at Vt and Vs as indicated in figs. 4 and 5. The same behaviour is obtainable also with LM's realized with leaks b=400 μm (or holes of $\phi$=400 μm in a copper layer) and needles of $\phi$=400 μm as wire-points (Vt= -1170 V, Vs= -1250 V).

With the α source set some millimetres above the LM, always in open room air, one can see with the oscilloscope a behaviour with the following features:

i) starting with the HV at more than 100 V below Vt the pulses due to α particles grow in amplitude and in counting rate as HV grows, while their duration grows with increasing b. They have all the amplitudes, from few mV up to a maximum (up to more than 100 mV in some cases). The anodic and cathodic pulse-pair, due to the detection of an α particle, are of opposite polarity, have the same amplitude and duration, are essentially in time coincidence with rise (fall) time of some ns. Furthermore these pulses (charges) are both, on the anode and on the cathode of the LM, essentially unipolar. The anodic and the cathodic channels are both very stable and bereft of spurious pulses. The counting rate is of few α pulses per second as expected. This is due to the fact that the effective volume of the LM is restricted to a narrow region near the anode-wire-point because of electron removal by negative ion formation in the open air [7].

ii) from Vt to Vs , the α pulses are superimposed to the above threshold pulses just described.

The detection of α particles was verified for every b indicated in figs. 3, 4 and 5.

Figs. 6, 7 and 8 show examples of the anodic and cathodic α pulses recorded by a LeCroy 9361 oscilloscope, under the geometry and working conditions indicated. Vα are the values of the HV at which the α particles were detected. Fig.7 shows also the effect of square pulses of 10 mV injected into the anodic pick-up through a 100 Ω resistor. The voltage amplification Vout/Vin of the pick-ups of fig.2 results to be ~3 (or 0.3mV/μA). The absence of substantial differentiation, along with the fact that the very small equivalent capacitance C, of both the LM

itself and the connecting wire to the pick-up, and the low impedance R represented by the sum of the two input impedance of the pick-ups of fig. 2 (100 Ω + 100 Ω) give rise to an RC time constant much smaller than the ion collection time, permit to say that in the anodic as well as in the cathodic pulses the rising current is due to electron component while the current peak declines (ion component) exponentially, or perhaps parabolically, and falls to zero as the last of the positive ion cloud was picked up by the cathode [8]. These circumstances give an idea about the gas multiplication and about the counting rate at which a single LM could be able to work.

The following preliminary observations were furthermore made:

a) for every value b of the leak Vs is higher the more equidistant the point is from the borders of the strips: moving the point off the center Vs decreases and can become lower than Vt preventing any practical result.

b) in any case the above threshold pulses don't take place and there are no practical results if the wire-point, in the LM, doesn't emerge into open air (or in gas) for a length equal to at least three or four times the point (wire) diameter.

c) Vt and Vs depend on the height z of the point, relative to the upper face of the strips. Fig.9 illustrates the trends of these dependences for a wire-point $\phi$=50 μm at b=300 μm. It shows also the rate of α pulses/s , and the maximum recorded amplitude of the pulses in mV , when for every position of the point the HV (Vα) was set just below Vt.

d) using the pillory of fig.1 with the two strips parallel to form a leak of b=200 μm and with two wire-points of $\phi$=20 μm the counting rate of the α pulses almost doubles when the distance from the two points, in the leak, is changed from 300 to 1200 μm (Vα=-930 V).

e) fig.10 shows the anodic and the cathodic α pulses from a wire-point of $\phi$=20 μm and b~400 μm at Vα= -930 V. Fig.11 shows the

pulses obtained with the previous LM in the same working conditions but with the input of the cathodic pick-up short-circuited to ground with a 100 pF capacitor. The fall time of the cathodic output pulses changes to a few ns : this means that the LM acts as a voltage generator with a rather low internal impedance in series.

## 4. The two-dimensional position sensitive detecting board

As a first approach to translate into practice the results just described the structure depicted in fig.12 was constructed.

In a sandwich made with two pieces of printed circuits board (glass-epoxy laminate, both ~10x10 $mm^2$ and 1 mm thick, with copper foils 37μm thick coating both sides) a matrix of nine holes of $\phi$=400 μm was drilled (pitch 1 mm).

One of the two external conducting-layers was divided into strips, separated by the nine holes. The other external conducting-layer was also divided into strips, perpendicular to the previous ones, but centred on the holes.

Nine needles, of nickel plated iron and $\phi$=400 μm, were inserted with their points well centred in the holes between the strips to form nine LM's. On the other external layer the needles passing in the middle of the strips were soldered to them and cut.

On the two internal copper-layers, adhering to each other, and forming an intermediate conducting-layer, the holes were reamed to prevent contact with the pass-through needles.

The structure, therefore, consists of a cathodic surface (**detecting surface**) with nine LM's (copper strips 37 μm thick, forming leaks b=400 μm with the points of the needles in the middle), of an **intermediate conducting layer** and of an anodic surface (**backplane**: strips in contact with the needles). Let us name this structure as the **L.N.L. structure** ( Laboratori Nazionali di Legnaro).

We verified , first of all, that each of the nine LM's were running with $\alpha$ particles. We then observed that during the running of a single LM the cathodic charge is shared by the two adjacent strips. This observation, along with that just reported in the previous point d), suggests that a suitable choice of the pitch of the LM's, in such a manner that the primary ionization strikes two or more LM's, allows to get an improved spatial resolution by using the centroid method or better the charge-ratio method for both the X and Y coordinates. This is possible because the LM's supply charges proportional to the primary ionization collected: this is what will be seen in a little while.

Figs. 13 and 14 report, in different time scales, the anodic and cathodic $\alpha$ pulses obtained, always in open room air, with the L.N.L structure at $V\alpha$=-1150 V. All the cathodic strips, as well as the anodic strips, were connected together.

Fig.15 shows the fast "kicks" pulses obtainable by connecting the intermediate layer of the L.N.L. structure directly to the base of the BFT 96 input transistor of an anodic pick-up (see fig.2). As can be seen in fig.15, some mismatching clearly occurred. Natheless it is possible to say that these kick pulses are the OR of the anodic and the cathodic pulses of the external surfaces (no matter how they were subdivided) offering a good trigger to "coordinate" them in a two-dimensional read-out system.

Moreover the intermediate layer limits the capacitive cross-talk (or shields electrostatically quite completely if grounded) between the two external surfaces.

An evaluation of the highest observed gas (air) multiplication gives a number of the order $4 \times 10^5$. This evaluation comes from taking into account the mean amplitude (~1mV) and the duration (~40 ns) of the observed above threshold pulses, obtained with the L.N.L. structure at Vt=-1170 V , assuming that these above threshold

pulses are due to avalanches induced by single electrons ejected from the cathodes by field emission (under investigation as it was said above). We used the formula G=VT/2AZe where G=gas multiplication, V=amplitude of the pulses (~1mV), T=duration of the ion collection process (~40 ns), A=electronic amplification (3), Z=input impedance of the pick-ups of fig.2 (100 Ω) and e is the electron charge. The factor 1/2 comes from the fact that we evaluate the mean current of the pulse to be equal to $i_{peak}/2=V/2AZ$.

## 5. The LM's behaviour in gas

In order to test the characteritics of the LM's behaviour in gas, and whether they are able to deliver charges proportional to the primary ionization collected, isobutane gas was used. As it was said above, due to electron removal by negative ion formation [7], the air is not a suitable gas for this purpose.

In fig.16 a typical cathodic α pulse recorded by a LeCroy 9054A oscilloscope is reported. The pulse was obtained with a LM of b=200 μm and wire-point ϕ=20 μm in 500 Torr of isobutane at Vα=-830 V. The good signal to noise ratio should be noted and the features of this pulse have to be compared with those of fig.7 obtained in open room air.

In order to undestand, first of all , the behaviour of a single LM and than, if the case, to test structures more complicated, we built with a piece of printed board ~10x10 $mm^2$, 1mm thick , and a hole of ϕ=400 mm , a single LM with the same size and with the same material of those used for the L.N.L. structure of fig. 12 (sample # 3 ). The needle was soldered on the backplane.

A mesh was put 10 mm above the sample # 3. It was able to support an $^{241}Am$ source, whose distance, from the sample # 3, resulted to be 15.7 mm. Negative HV(Vmesh), through an RC filter (100kΩ, 4.7nF), was applied to this mesh. With this experimental set-up and working in 575 Torr of isobutane it was noticed that, setting Vα=-1100 V, as Vmesh was rising from -1100 V up to -1700 V the amplitude of the α pulses was increasing. As a consequence, the α peak in the energy distribution moved to higher channels in the MCA (multichannel analyzer : Silena Mod. 7934-4096)

without substantial variations of the FWHM (full width at half maximum) of the peaks. Fig.17 shows the overlap of two energy distributions ($V\alpha$=-1100 V in 575 Torr of isobutane for both spectra) setting Vmesh=-1100 V and Vmesh=-1700 V respectively. This observed behaviour is similar to that of a pulser in calibrating a nuclear spectrometer : the FWHM is set by the noise of the electronic chain, but it is the same for all the possible peaks in the dynamic range of the MCA, while the increasing charge injected in the preamplifier (which, if normalized, represents the energy) is set by the increasing amplitude of the pulses. In our case the FWHM is set mainly by the gas multiplication of the LM ($V\alpha$=-1100 V) and it is almost the same for all the possible peaks, while the increasing charge injected in the LM (or collected by the LM) is set by increasing Vmesh. The fact that the "columnar recombination" [9] decreases by increasing Vmesh is evident. The LM provides, therefore, charges proportional to the primary ionization collected.

Fig.18 shows the energy distribution of $\alpha$ particles from an $^{241}$Am source ($V\alpha$=-1000 V, Vmesh=-1600 V in 591 Torr of isobutane) still using sample # 3. An energy resolution of about 8% FWHM was obtained. Fig.19 shows the energy distribution of the $\alpha$ particles from a three-peak $\alpha$ source Pu(5.155 MeV) +Am(5.485 MeV)+Cm(5.806 MeV)] : $V\alpha$=-1100 V, Vmesh=-1100 V in 585 Torr of isobutane always with the sample # 3. The latter indicates that the energy resolution is near the limit to resolve the three peacks.

Since the $^{241}$Am as well as the 3-peak $\alpha$ sources were both deposited on a metallic disk, it was possible to apply a negative HV (Vsource) directly to them. In fig.20 is shown the energy distribution obtained with the $^{241}$Am $\alpha$ source set ~16 mm above the L.N.L. structure in 600 Torr of isobutane at $V\alpha$=-1100 V and Vsource=-1600 V. The latter is the sum of the spectra of the nine LM's working together at the same $V\alpha$ but with different gas multiplication (due to little differences in the mechanical sizes of the LM's). This observation suggests that there

are two possible ways for reducing or for equalizing this spread of the gas multiplication. The first consists , once chosen the proper sizes of the LM's, in reproducing all points with the same size and position (height : see fig 9),i.e., with the lowest possible per cent error , as can be understood by analysing the data reported in figs. 3, 4, 5 and 9. From the latter figs. it is also possible to understand that the per cent error which can be accepted in reproducing the size b of the leaks (or for the $\phi$ of the holes) is a few less mandatory than that needed for the points. All this, clearly, could be achieved by an industrial production, rather than by the handicraft we constructed. The second way consists in reading all the strips singularly and to equalize the recorded data off-line.
Rising $V\alpha$=-1230 V and Vsource=-2500 V in 608 Torr of isobutane the $\alpha$ pulses shown in fig.21 and 22, in different time scales, were recorded with the same L.N.L. structure . The saturation of the anodic pick-up is evident. Always with the same structure anodic and cathodic $\alpha$ pulses were recorded at various pressures in isobutane down to 15 Torr ($V\alpha$=-470 V at 15 Torr).

A mesh was set above the sample # 3 (4.1 mm spacing) working at the same HV($V\alpha$) of the cathode and the three-peak $\alpha$ source was set 19.2 mm above the sample. This mesh was decoupled from the cathode of the LM through an RC filter (100 k$\Omega$,4.7 nF). With $V\alpha$=-1400 V in 618 Torr of isobutane no pulses were noticeable with Vsource below -1500-1600 V. In fig.23 (618 Torr isobutane, $V\alpha$=-1400 V, Vsource=-2400 V) clusters of electrons (avalanches) induced by the primary ionization striking the LM at subsequent times are distinguishable. This result constitues further evidence that the LM's are able to deliver charges whose formation is due to the continuous collection and multiplication of the primary ionization at subsequent times, i.e.,the LM's are able to deliver charges proportional to the primary ionization collected.

In fig. 24 and 25 are shown some anodic and cathodic pulses and the pulse height distribution obtained setting a $^{55}$Fe source ~2mm above the sample # 3 working at Vx=-1200 V in 600 Torr of isobutane.

With these experimental conditions the absorbed X ray of 5.9 KeV from the $^{55}Fe$ source gives rise up to ~200 electrons of primary ionization. Taking into account the maximum recorded amplitude (~100 mV) of these pulses, the duration of the ion collection process (~40 ns.) and that this maximum amplitude is due to ~200 primary electrons, we find again, as the gas multiplication, a number ($2x10^5$) which is not so much different from that above evaluated. Furthermore the fact that the distribution of fig. 25 represents, as a function of the MCA channels, the probability (not normalized) of these primary electrons to be collected, from one (or few) up to ~200, put in evidence that the LM's are not only able to detect heavily ionizing particles, like $\alpha$ particles, but also weakly and minimum ionizing particles, like X rays or $\beta$ particles or other, delivering pulses quite large in amplitude (see fig.24) and without corona or other secondary noises. In figs. 26 and 27 are shown the anodic and cathodic pulses and their pulse height distribution obtained setting a $^{14}C$ $\beta^-$ source (endpoint 156.5 KeV) ~2mm above the sample #3 at $V\beta$=-1200V in 600 Torr of isobutane.

All previous distributions were recorded by sending the pulses, delivered from one of the pick-ups of fig.2, to the input of a main amplifier (Silena Mod. 7612/L) with a shaping time of 250 ns. No significant differences in the energy distribution were noticed if obtained using the anodic or the cathodic pulses or those from a charge preamplifier (Ortec 142PC) replacing the anodic pick-up. In the latter case, however, the pulses became longer, preventing a possible high counting rate.

In order to have an evaluation about the detection efficiency, $\alpha$ particles were detected with a silicon detector and with a LM of b=200 $\mu$m and $\phi$=20 $\mu$m (fig.16) with the source set at the same distance above the two detectors ( $V\alpha$=-830 V in 500 Torr of isobutane). On the basis of the counting rate obtained with each detector, and the known area of the silicon detector, it was estimated that the LM was efficient in a surface of about $1mm^2$.

All the pulses as well as the distributions shown in the figures of the present work were obtained using the pick-ups of fig.2.

At this point it is worthwhile to draw attention to the fact that a structure like that of fig.12 can resolve the problem of the multihit in two dimensions if all the strips are read singularly. If two ionizing radiations (or two clusters of primary ionization) in coincidence (within a resolving time) strike the detecting surface at two different points ($X_a$, $Y_a$) and ($X_b$, $Y_b$) clearly one has two "hits" and two "ghosts" (Xa,Yb and Xb,Ya). But it is possible to resolve this ambiguity comparig the four signals. The hits have for X and Y a signal-pair with the same features and characteristics (except for polarity). The ghosts have for X and Y two signals which are different for the time and/or for the shape and/or for the charge. If the two ionizing radiations in coincidence have in common one coordinate, that is for instance ($X_a$, $Y_a$) and ($X_a$, $Y_b$), in the common coordinate $X_a$ there is pile-up of the pulses causing a possible loss of the energy (charge) and time information; however the energy (charge) and time information are conserved equal and separated in $Y_a$ and in $Y_b$. All this is a direct consequence of the fact that for each gas ionizing radiation (or cluster of primary ionization) detected by a LM, the wire-point and the leak (strips) of this LM both supply the same energy (charge) and time information through a pulse-pair which are identical in all features and characteristics, except for polarity.

Finally the wire-points of the LM's can be read one by one or in groups in direct connection (DC) if the cathode(s) are supplied with negative HV.

## CONCLUSIONS

It was put in evidence the possibility to use points, arranged in particular microstructures, to detect gas ionizing radiations avoiding the corona noise and the Geiger regime, with high gas multiplication and consequently with high output pulses on low impedance with a rapid

risetime. These microstructures act like voltage generators with a rather low internal impedance in series. The ratio $Q_X/Q_Y$ of each charge-pair supplied by these microstructures for each detected ionizing radiation is 1 and both $Q_X$ and $Q_Y$ charges of each pair give the same energy and time information. The energy resolution FWHM with $\alpha$ particles is good. There is evidence that the LM's are able to detect weakly and minimum ionizing particles.

The possibility of communication between two conducting surfaces, via "conductivity" through the wire-points of the microstructures was verified with the L.N.L. structure (fig.12). The two surfaces, which need not be parallel and flat, can be subdivided, not necessarily, in straight orthogonal strips, to form a sensitive position two-dimensional readout.

Between the two "active surfaces" it is possible to insert a third conducting layer to limit (or practically suppress) the capacitive cross-talk between the two external active surfaces. Moreover this intermediate layer can give a very fast trigger to "coordinate" the charges (pulses) of the two external surfaces and to govern the data acquisition system.

When in a structure like that of fig. 12 all strips are read singularly and position, energy (charge) and time information are required, one can resolve the multihit problem in two-dimensions.

All this work is finalized to digital radiography.

We are now trying to realize the described LM's and a structure like that of fig.12 using photosensitive polyimid and galvanic growth.

The authors are in debt to Dr. G. Prete of INFN Legnaro Laboratories for the help given in some measurement and in the evaluation of the results obtained. Are also in debt to Profs. G. Della Mea and U. Gastaldi of INFN Legnaro Laboratories for discussions during the development of this work. Many thanks to Prof. B. Lombardi, authors' brother, of University of Pittsburgh-School of Medicine-Department of Pathology for the help and the skilful suggestions given during the development of this work.

FIGURE CAPTIONS

Fig.1 - Experimental set-up

Fig.2 - Cathodic and anodic pick-ups

Fig.3 - Vt and Vs as functions of b (in μm) for a tungsten wire-point $\phi$=20 μm.

Fig.4 - Vt and Vs as functions of b (in μm) for a tungsten wire-point $\phi$= 10 μm.

Fig.5 - Vt and Vs as functions of b (in μm) for a tungsten wire-point $\phi$=50 μm.

Fig.6 - Anodic and cathodic α pulses obtained with a tungsten wire-point $\phi$=20 μm, b=100 μm at Vα=-760V. Ch.1-20 ns/cm, 5mV/cm. Ch. 2-20 ns/cm, 10 mV/cm.

Fig.7 - Anodic and cathodic α pulses obtained with a tungsten wire-point $\phi$= 20 μm, b=200 μm at Vα=-830V. Square pulses of 10 mV through a resistor of 100 Ω are injected in the anodic pick-up. Ch.1-20 ns/cm, 10 mV/cm. Ch.2-20 ns/cm, 20 mV/cm.

Fig.8 - Anodic and cathodic α pulses obtained with a tungsten wire-point $\phi$=50 μm, b=300 μm at Vα=1070 V.
Ch.1-10 ns/cm, 10 mV/cm. Ch2-10 ns/cm,10 mV/cm .

Fig.9 - Vt ( + ), Vs ( O ), max. amplitude of the α pulses ( Δ) and number of α pulses/sec. ( ❑ ) as functions of the height z (in μm) of the point to respect the upper surface of the strips. Tungsten wire-point $\phi$=50 μm, b=300 μm.

Fig.10- Anodic and cathodic α pulses obtained with a tungsten wire-point $\phi$=20 μm, b~400 μm at Vα=-930 V.
Ch.1-10 ns/cm, 10 mV/cm. Ch.2-10 ns/cm, 10 mV/cm.

Fig.11- Pulses obtained with the same LM used for the pulses of fig.10 in the same working conditions but with the input of the cathodic pick-up short-circuited to ground with a 100 pF capacitor. Vα=-930 V. Ch.1-10 ns/cm, 10 mV/cm.
Ch.2-10 ns/cm, 10 mV/cm.

Fig.12- The two-dimensional readout position sensitive detecting board: the L.N.L. structure.

Fig13- Anodic and cathodic α pulses obtained in open air with the L.N.L. structure . Vα=-1150 V. Ch.1-20 ns/cm, 20 mV/cm.
Ch.2-20 ns/cm, 20 mV/cm.

Fig.14- The same pulses of fig.13 in a different time scale.
Ch.1-1 μs, 20 mV/cm. Ch.2-1 μs, 50 mV/cm.

Fig.15- In Ch.2 the fast "or kicks" of the intermediate layer.
Ch.1-20 ns/cm, 20 mV/cm. Ch.2-20 ns/cm,10 mV/cm.

Fig.16- A typical anodic α pulse recorded with a tungsten wire-point $\phi$=20 μm, b=200 μm in 500 Torr of isobutane at Vα=-830 V.
20 ns/cm, 20 mV/cm.

Fig.17- Overlap of two energy distributions obtained setting Vmesh=-1100 V and Vmesh=-1700 V in 575 Torr of isobutane.

Fig.18- Energy distribution of α particles from an $^{241}$Am source.
Vα=-1000 V, Vmesh=-1600 V in 591 Torr of isobutane.

Fig.19- Energy distribution of α particles from a three peaks source. Vα=-1100 V, Vmesh=-1100 V in 585 Torr of isobutane.

Fig.20- Energy distribution of α particles from an $^{241}Am$ source obtained with the L.N.L. structure (nine LM's working together). Vα=-1100 V, Vsource=-1600 V in 600 Torr of isobutane.

Fig.21- Anodic and cathodic α pulses obtained with the L.N.L. structure in 608 Torr of isobutane at Vα=-1230 V and Vsource=-2500V. Ch.1-20 ns/cm, 200 mV/cm. Ch.2-20 ns/cm, 200 mV/cm.

Fig.22- The same pulses of fig.21 in a different time scale. Ch.1-1 μs/cm, 200 mV/cm. Ch.2-1 μs/cm, 200 mV/cm.

Fig.23- Anodic and cathodic pulses obtained with the sample # 3 in 618 Torr of isobutane.Vα=1400V, Vsource=-2400V. Ch.1-0.1 μs/cm, 2mV/cm. Ch.2-0.1 μs/cm, 2 mV/cm. Clusters of electrons (avalanches) induced by the primary ionization striking the LM at subsequent times are distinguishable.

Fig.24 Anodic and cathodic pulses obtained with a $^{55}Fe$ source at Vx=-1200V in 600 Torr of isobutane. Ch.1-20 ns/cm, 20 mV/cm. Ch.2-20 ns/cm, 20 mV/cm.

Fig.25 Pulse height distribution of the pulses obtained with the $^{55}Fe$ source.

Fig.26 Anodic and cathodic pulses obtained with a $^{14}C$ $\beta^-$ source. Ch.1-20 ns/cm, 20 mV/cm. Ch.2-20 ns/cm, 20 mV/cm.

Fig.27 Pulse height distribution of the pulses obtained with the $^{14}C$ source.

REFERENCES

[1] W.Y. Chang and S. Rosemblum, Phys. Rev. 67 (1945) 222
[2] G. Comby, Ph. Mangeot, J. Tichit, H. de Lignieres, J.F. Chalot et P. Monfray, Nucl. Instr. and Meth. 174 (1980) 77
[3] A. Oed, Nucl. Instr. and Meth A263 (1988) 351
[4] M.R. Bishai, E.K.E. Gerndt, I.P.J. Shipsey, P.N. Wang, Proceedings of the International Workshop on micro-strip gas chambers -Legnaro, october 13-14 ,1994-p.12
[5] M. Lombardi, Tan Jilian, R. Potenza, V. D'Amico, Nucl. Instr. and Meth. A 238(1985)422
[6] G.W.Trichel, Phys. Rev. 54 (1938) 1078
[7] Takaniko AOYAMA and Tamaki WATANABE Nucl. Instr. and Meth. 197(1982)357-363
[8] L.B. Loeb, Electrical Coronas, Their basic Physical mechanism-University of California Press-Berkeley and Los Angeles-1965-p.417.
[9] G.F. Knoll, Radiation Detection And Measurements-John Wiley & Sons-1979-p.15

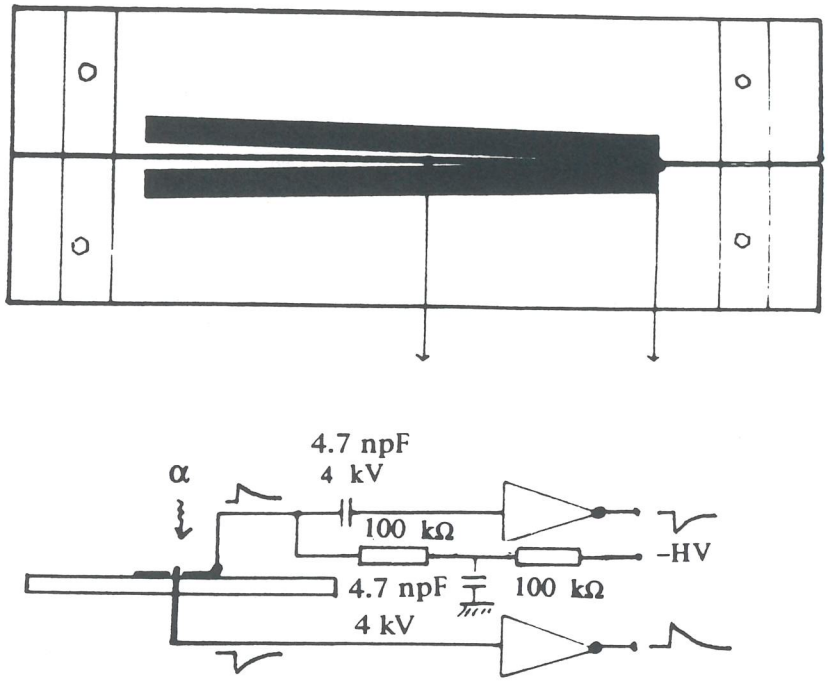


Fig. 1

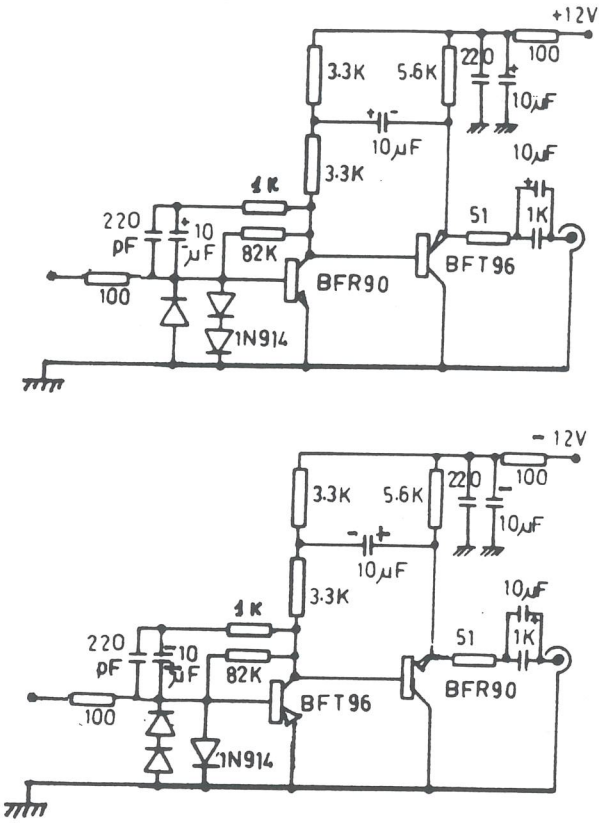
+12V
3.3K
5.6K
220
100
10µF
10µF
10µF
3.3K
1K
220
pF
10
µF
82K
51
1K
BFR90
BFT96
100
1N914
- 12V
3.3K
5.6K
220
100
10µF
10µF
10µF
3.3K
1K
220
pF
10
µF
82K
51
1K
BFT96
BFR90
100
1N914

Fig. 2

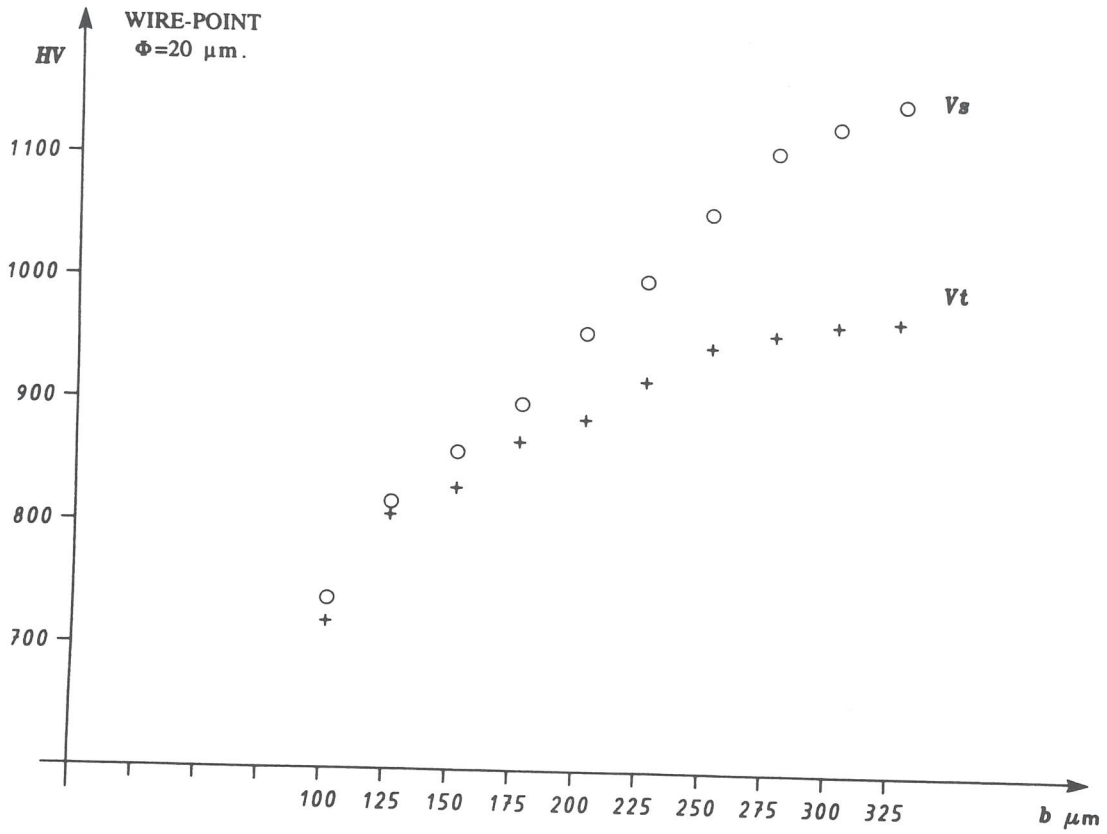
WIRE-POINT
Φ=20 µm.
HV
1100
1000
900
800
700
Vs
Vt
100
125
150
175
200
225
250
275
300
325
b µm

Fig. 3

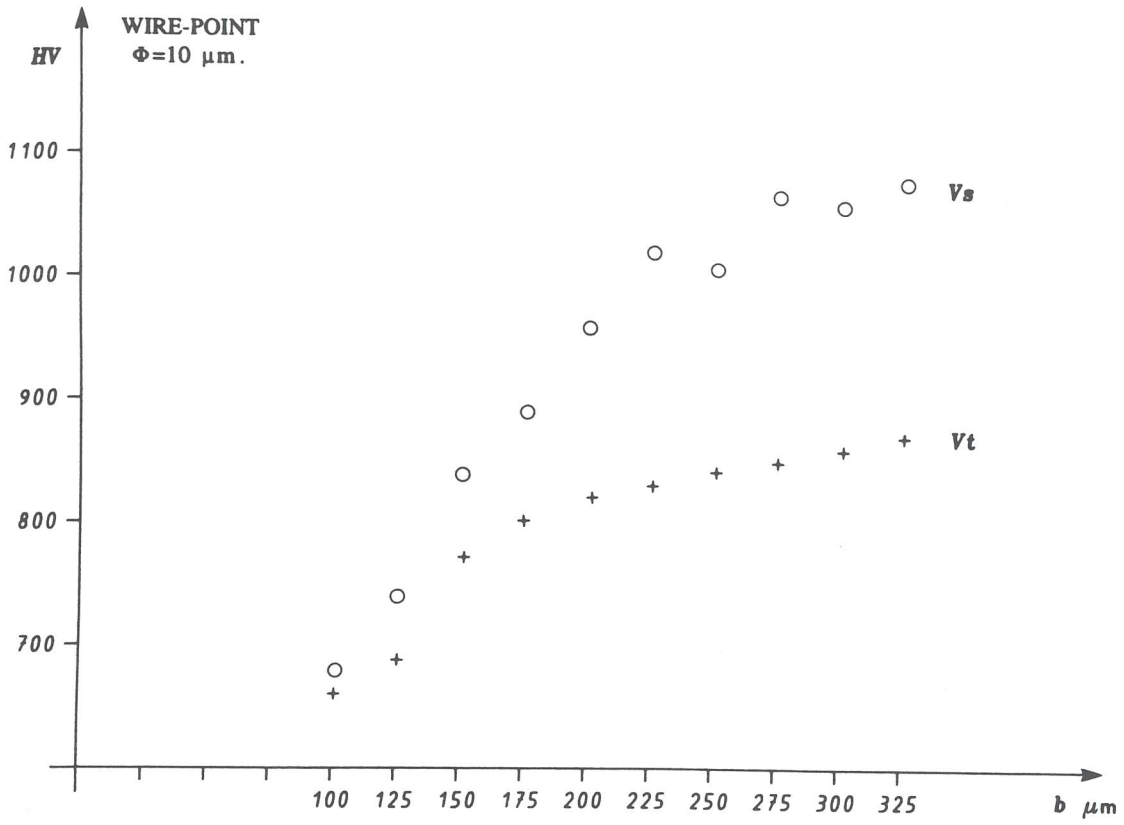
WIRE-POINT
Φ=10 µm.
HV
1100
1000
900
800
700
Vs
Vt
100
125
150
175
200
225
250
275
300
325
b µm

Fig. 4

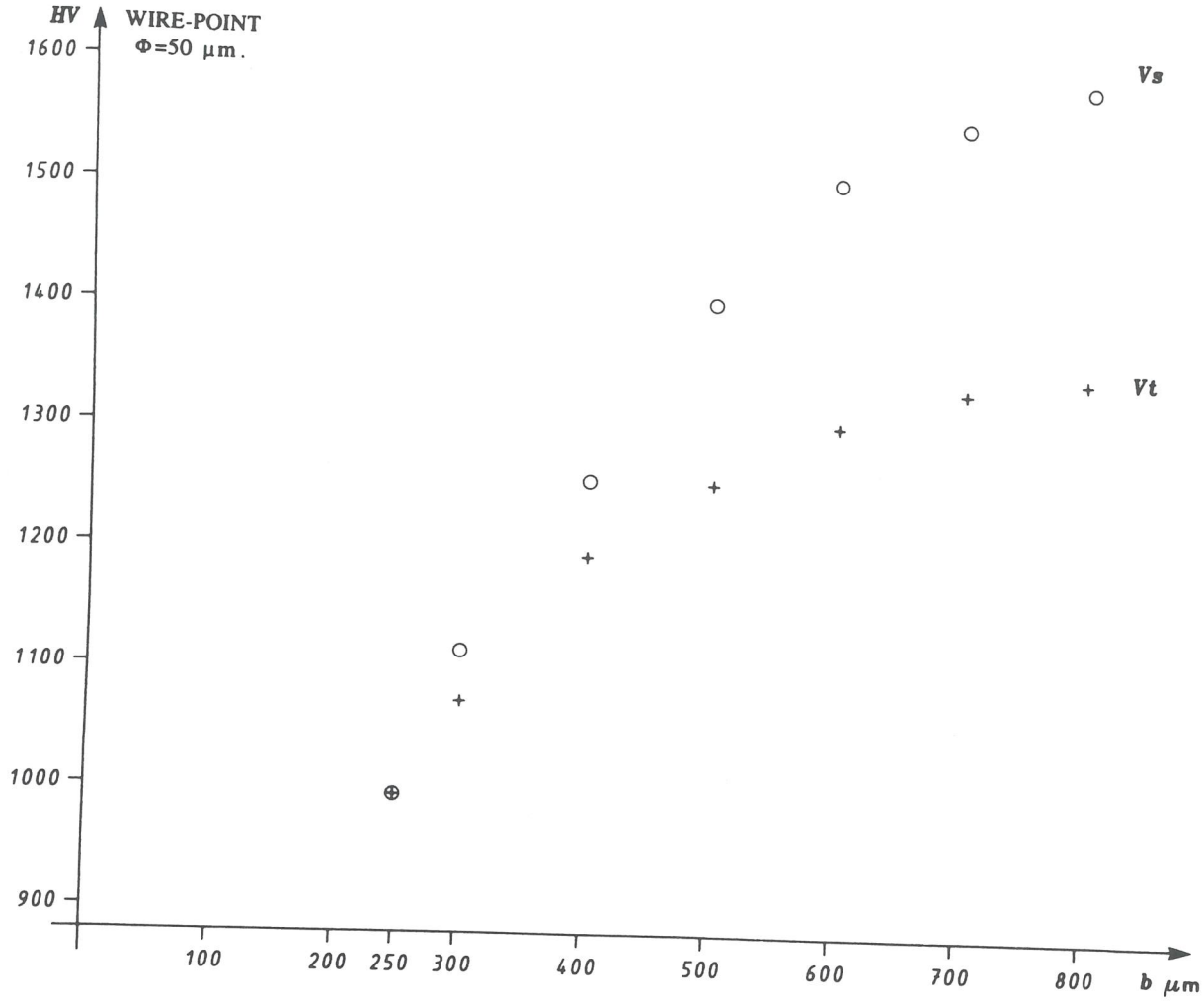
HV
WIRE-POINT
Φ=50 µm.
1600
1500
1400
1300
1200
1100
1000
900
Vs
Vt
100
200
250
300
400
500
600
700
800
b µm

Fig. 5

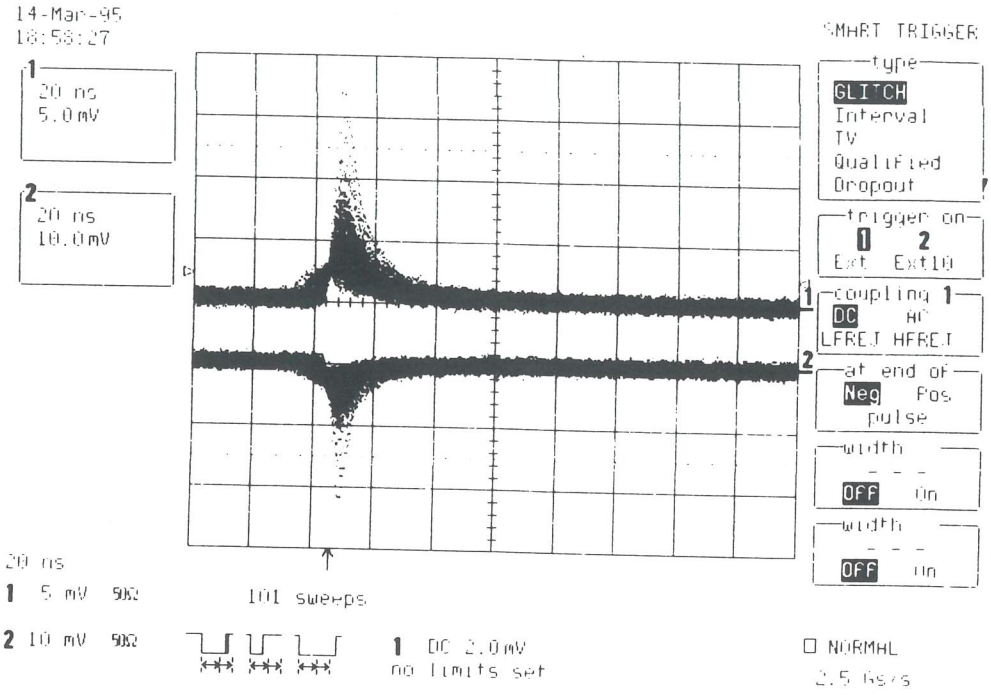
14-Mar-95
18:58:27
SMART TRIGGER
type
GLITCH
Interval
TV
Qualified
Dropout
trigger on
1 2
Ext Ext10
coupling 1
DC AC
LFREJ HFREJ
at end of
Neg Pos
pulse
width
Off On
width
Off On
1
20 ns
5.0 mV
2
20 ns
10.0 mV
20 ns
1 5 mV 50Ω
2 10 mV 50Ω
101 sweeps
1 DC 2.0 mV
no limits set
NORMAL
2.5 GS/s

Fig. 6

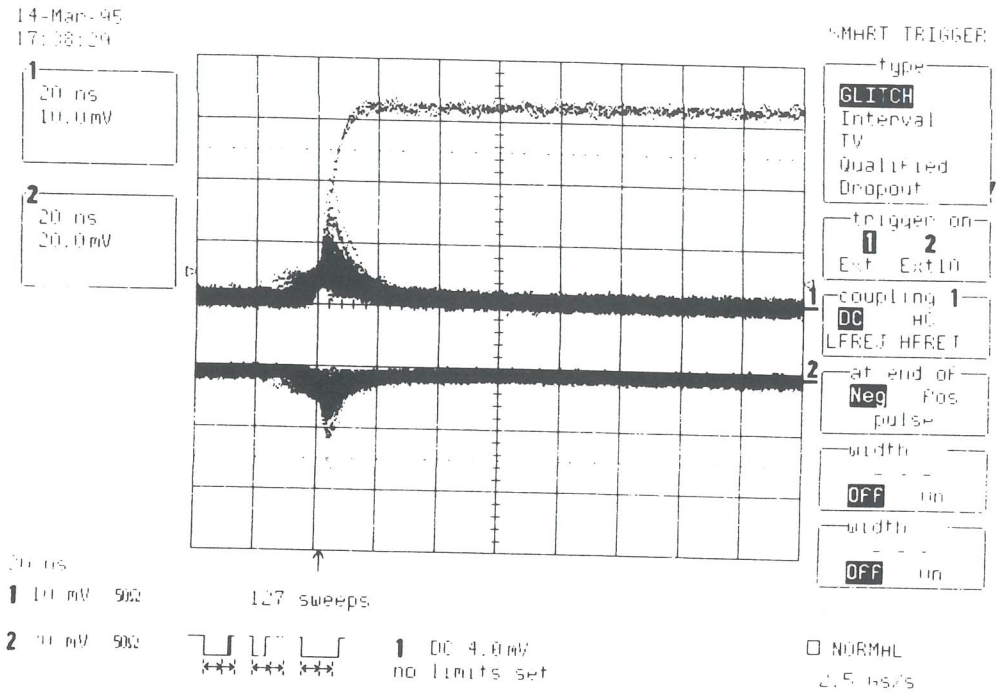
14-Mar-95
17:38:29
SMART TRIGGER
type
GLITCH
Interval
TV
Qualified
Dropout
trigger on
1 2
Ext Ext10
coupling 1
DC HF
LFREJ HFREJ
at end of
Neg Pos
pulse
width
OFF
width
OFF
20 ns
1 20 ns
10.0 mV
2 20 ns
20.0 mV
127 sweeps
1 DC 4.0mV
no limits set
NORMAL
2.5 ns/s

**Fig. 7**

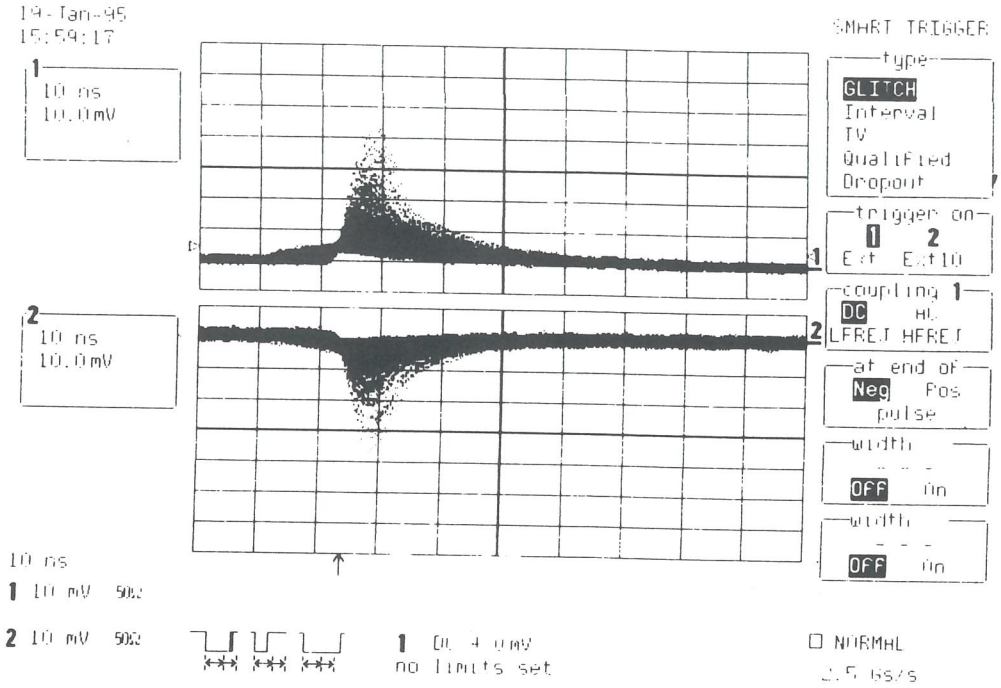
19-Jan-95
15:59:17
SMART TRIGGER
type
GLITCH
Interval
TV
Qualified
Dropout
trigger on
1 2
Ext Ext10
coupling 1
DC HF
LFREJ HFREJ
at end of
Neg Pos
pulse
width
Off
width
Off
1
10 ns
10.0mV
2
10 ns
10.0mV
10 ns
1 10 mV
2 10 mV
1 DC 4.0mV
no limits set
NORMAL

**Fig. 8**

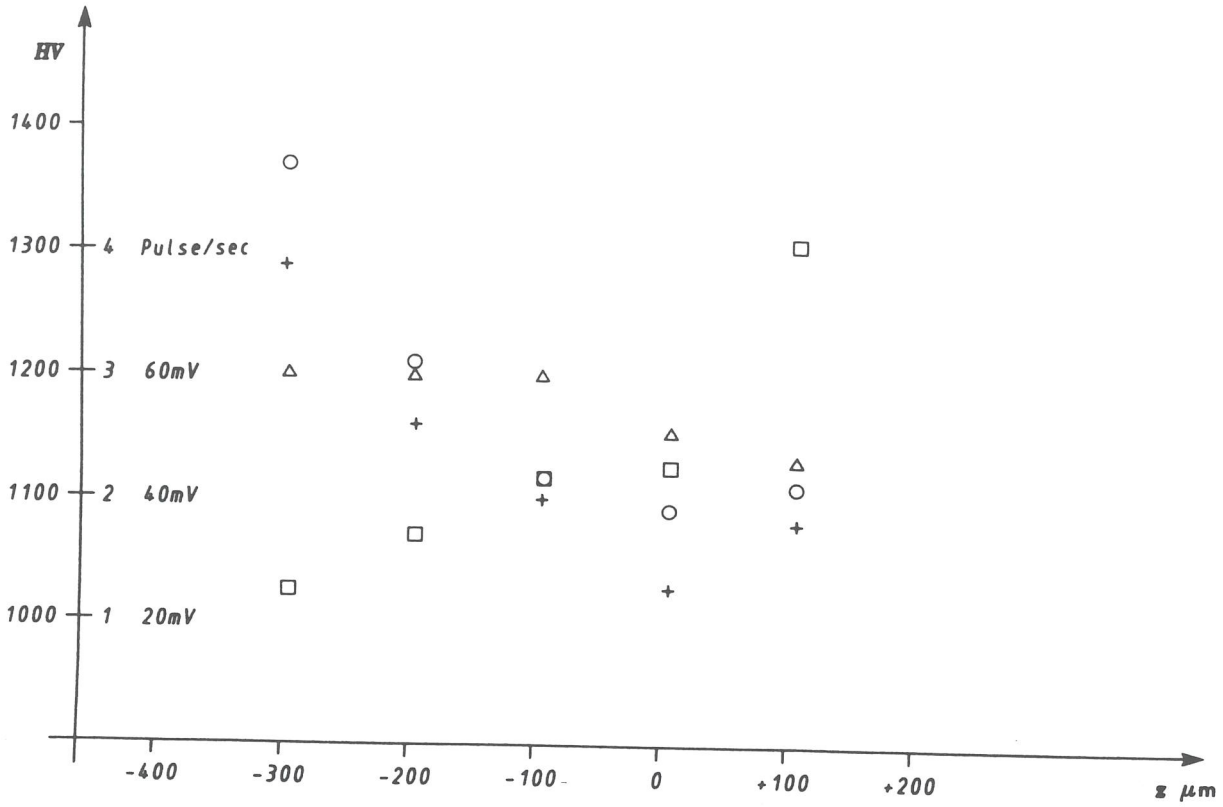
HV
1400
1300
4 Pulse/sec
1200
3 60mV
1100
2 40mV
1000
1 20mV
-400
-300
-200
-100
0
+100
+200
z µm

**Fig. 9**

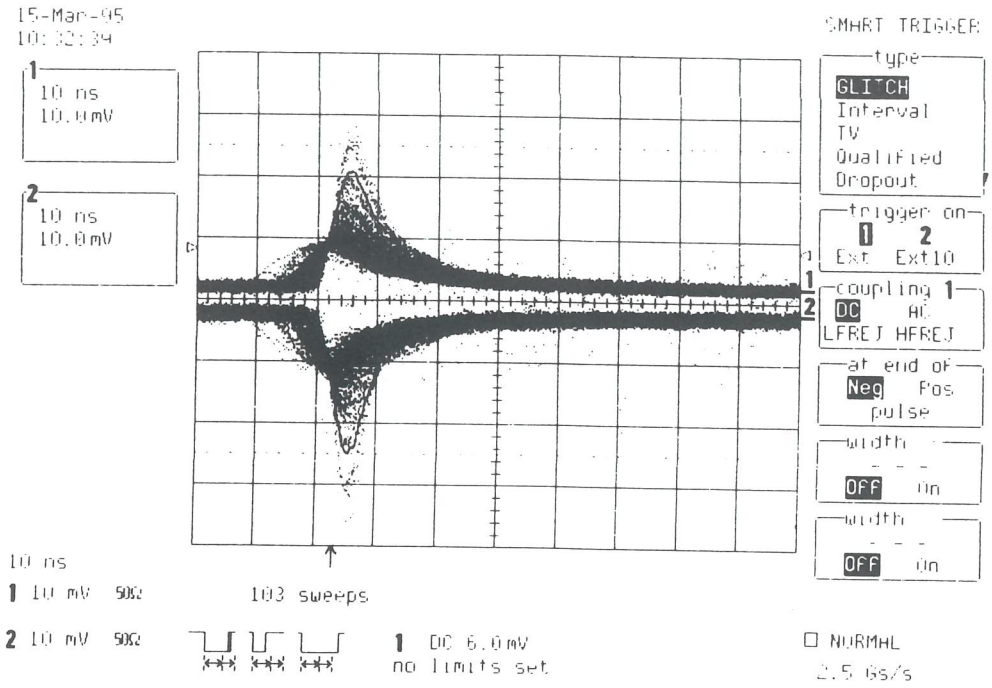
15-Mar-95
10:32:34
SMART TRIGGER
type
GLITCH
Interval
TV
Qualified
Dropout
trigger on
1 2
Ext Ext10
coupling 1
DC AC
LFREJ HFREJ
at end of
Neg Pos
pulse
width
Off On
width
Off On
1
10 ns
10.0mV
2
10 ns
10.0mV
10 ns
1 10 mV 50Ω
2 10 mV 50Ω
103 sweeps
1 DC 6.0mV
no limits set
NORMAL
2.5 GS/s

**Fig. 10**

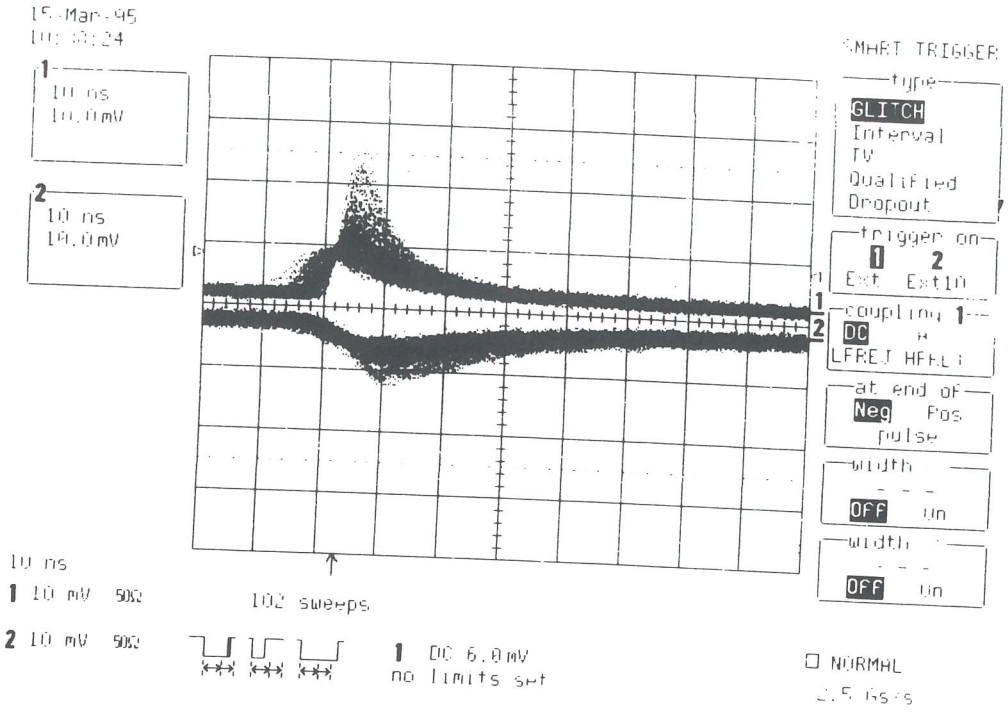
15-Mar-95
SMART TRIGGER
type
GLITCH
Interval
TV
Qualified
Dropout
trigger on
1 2
Ext Extin
coupling 1
DC
LFREJ HFREJ
at end of
Neg Pos
pulse
width
OFF On
width
OFF On
10 ns
1 10 mV 50Ω
2 10 mV 50Ω
102 sweeps
1 DC 6.0mV
no limits set
NORMAL

**Fig. 11**

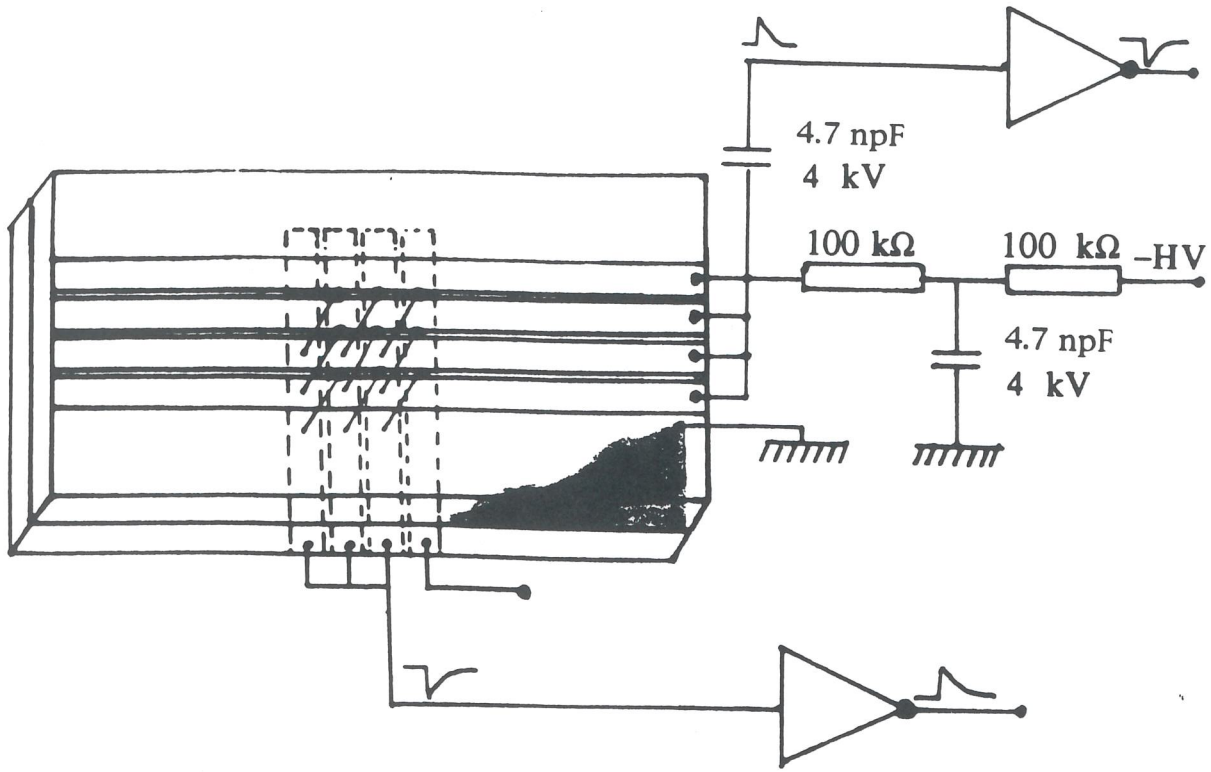


Fig. 12

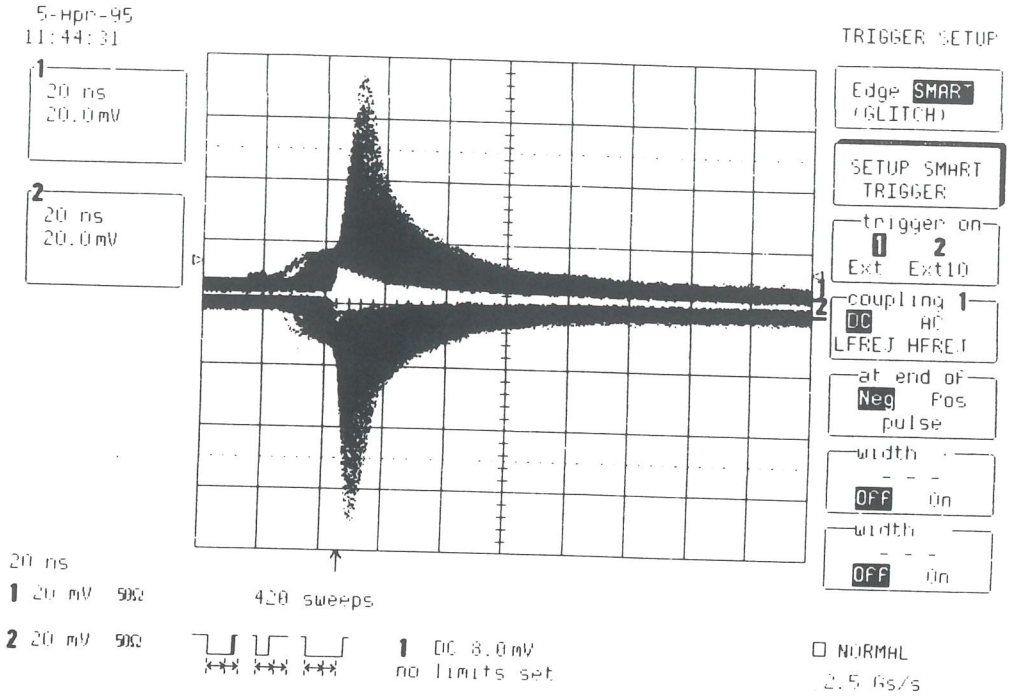
5-Apr-95
11:44:31
TRIGGER SETUP
1
20 ns
20.0mV
2
20 ns
20.0mV
Edge SMART
(GLITCH)
SETUP SMART
TRIGGER
trigger on
1 2
Ext Ext10
coupling 1
DC AC
LFREJ HFREJ
at end of
Neg Pos
pulse
width
OFF On
width
OFF On
20 ns
1 20 mV 50Ω
2 20 mV 50Ω
420 sweeps
1 DC 8.0mV
no limits set
NORMAL
2.5 Gs/s

Fig. 13

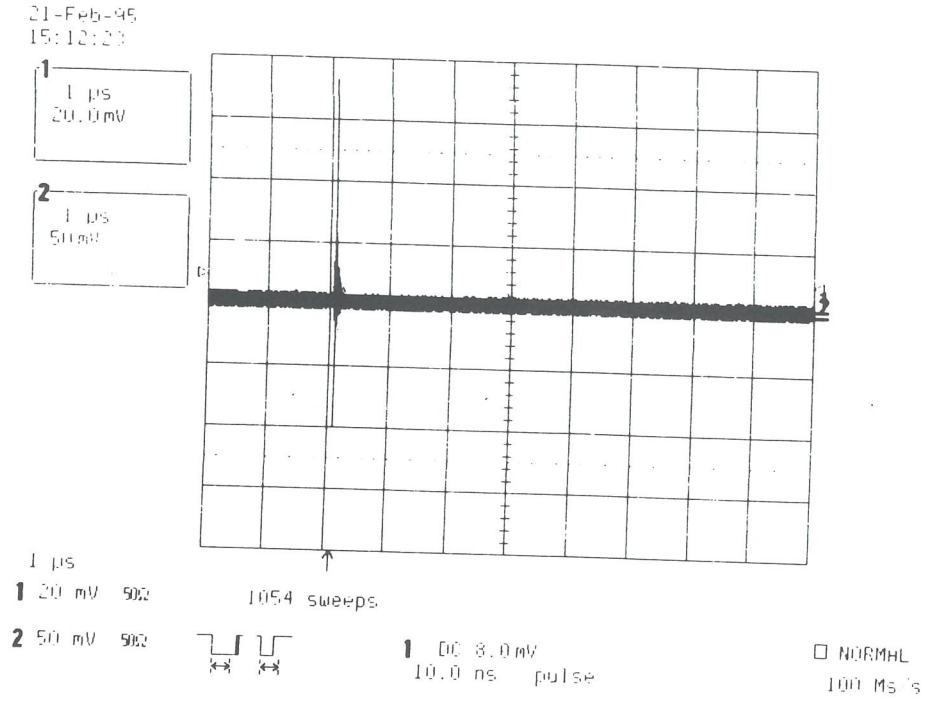
21-Feb-95
15:12:23
1
1 µs
20.0 mV
2
1 µs
50 mV
1 µs
1 20 mV 90Ω
2 50 mV 90Ω
1054 sweeps
1 DC 8.0 mV
10.0 ns pulse
NORMAL
100 Ms/s

**Fig. 14**

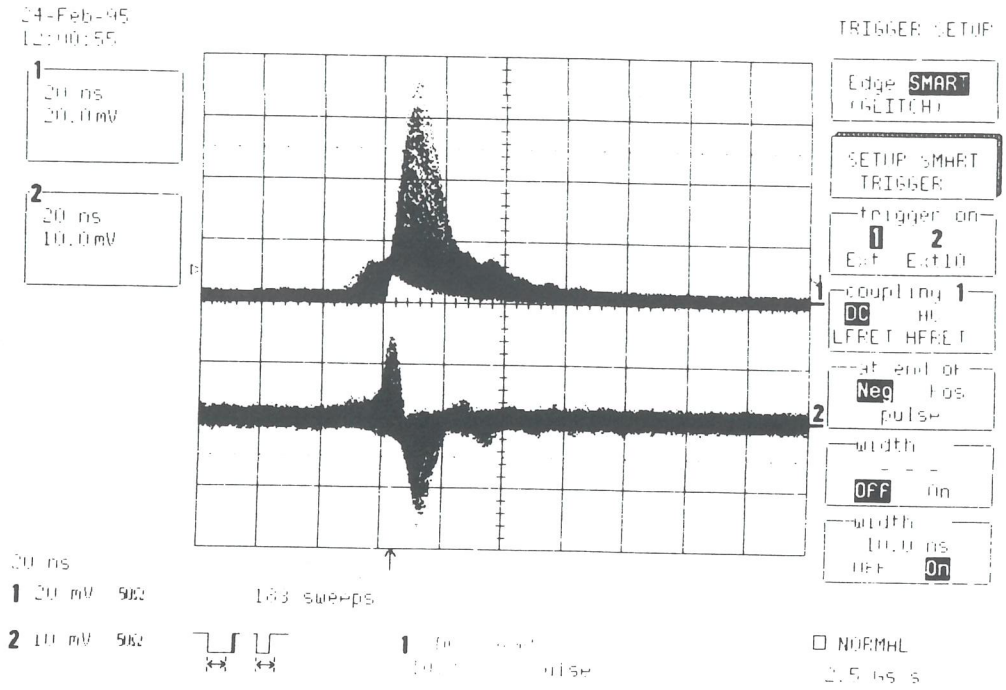
TRIGGER SETUP
Edge SMART
SETUP SMART
TRIGGER
trigger on
1 2
coupling 1
DC HF
Neg Pos
pulse
width
Off On
183 sweeps
NORMAL

Fig. 15

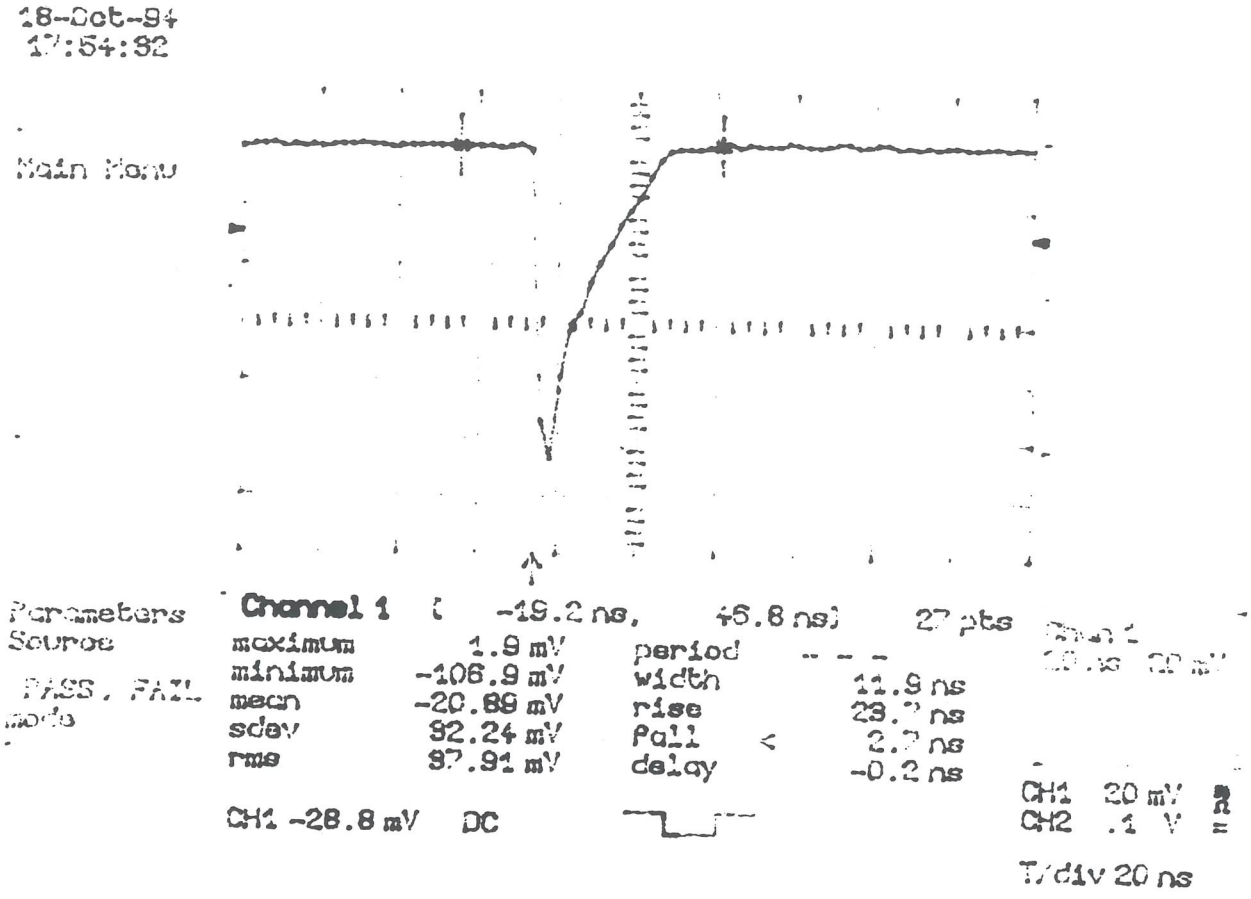
18-Oct-94
17:54:32
Main Menu
Parameters
Source
PASS, FAIL
mode
Channel 1 ( -19.2 ns, 46.8 ns) 27 pts
maximum 1.9 mV
minimum -106.9 mV
mean -20.89 mV
sdev 92.24 mV
rms 97.91 mV
period - - -
width 11.9 ns
rise 23.2 ns
fall < 2.2 ns
delay -0.2 ns
CH1 -28.8 mV DC
CH1 20 mV
CH2 .1 V
T/div 20 ns

Fig. 16

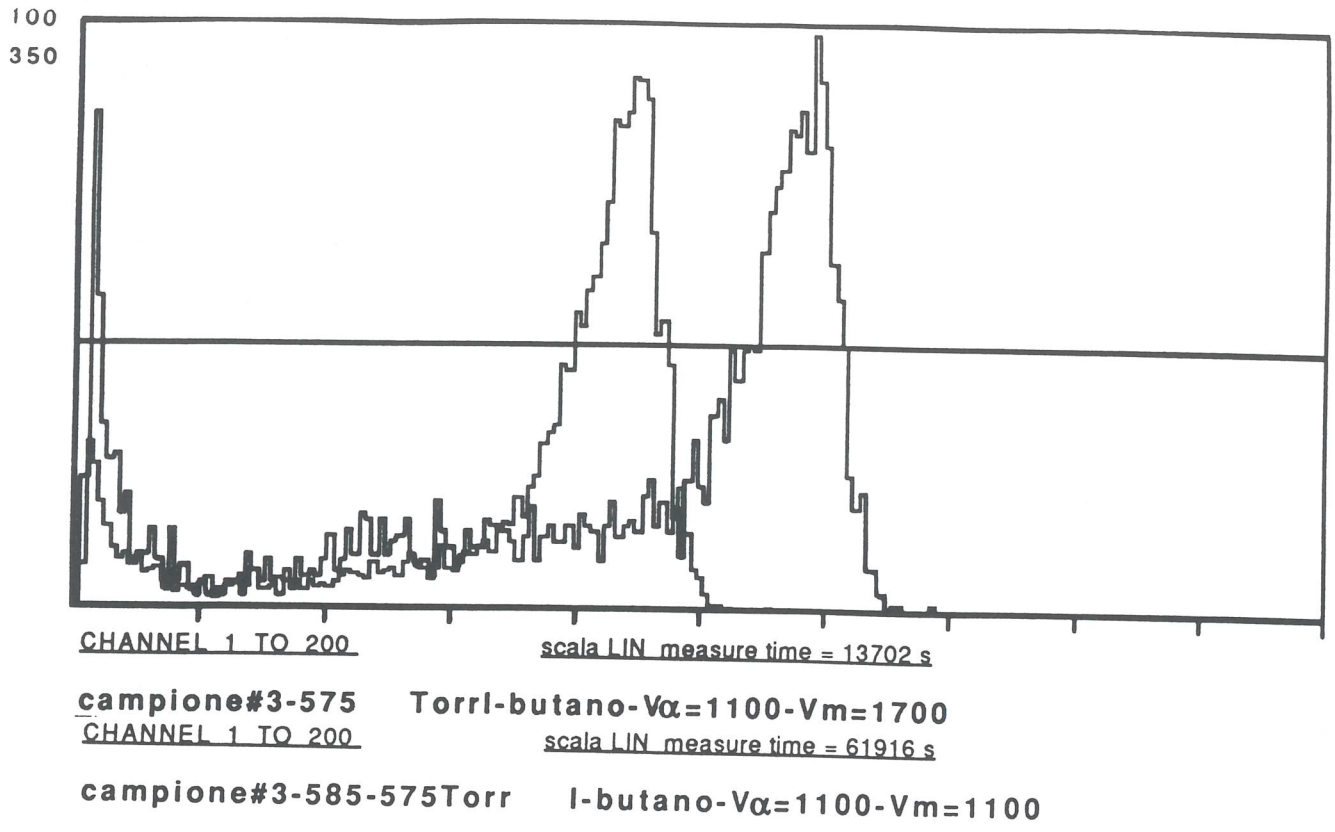
100
350
CHANNEL 1 TO 200
scala LIN measure time = 13702 s
campione#3-575 Torrl-butano-Vα=1100-Vm=1700
CHANNEL 1 TO 200
scala LIN measure time = 61916 s
campione#3-585-575Torr l-butano-Vα=1100-Vm=1100

Fig. 17

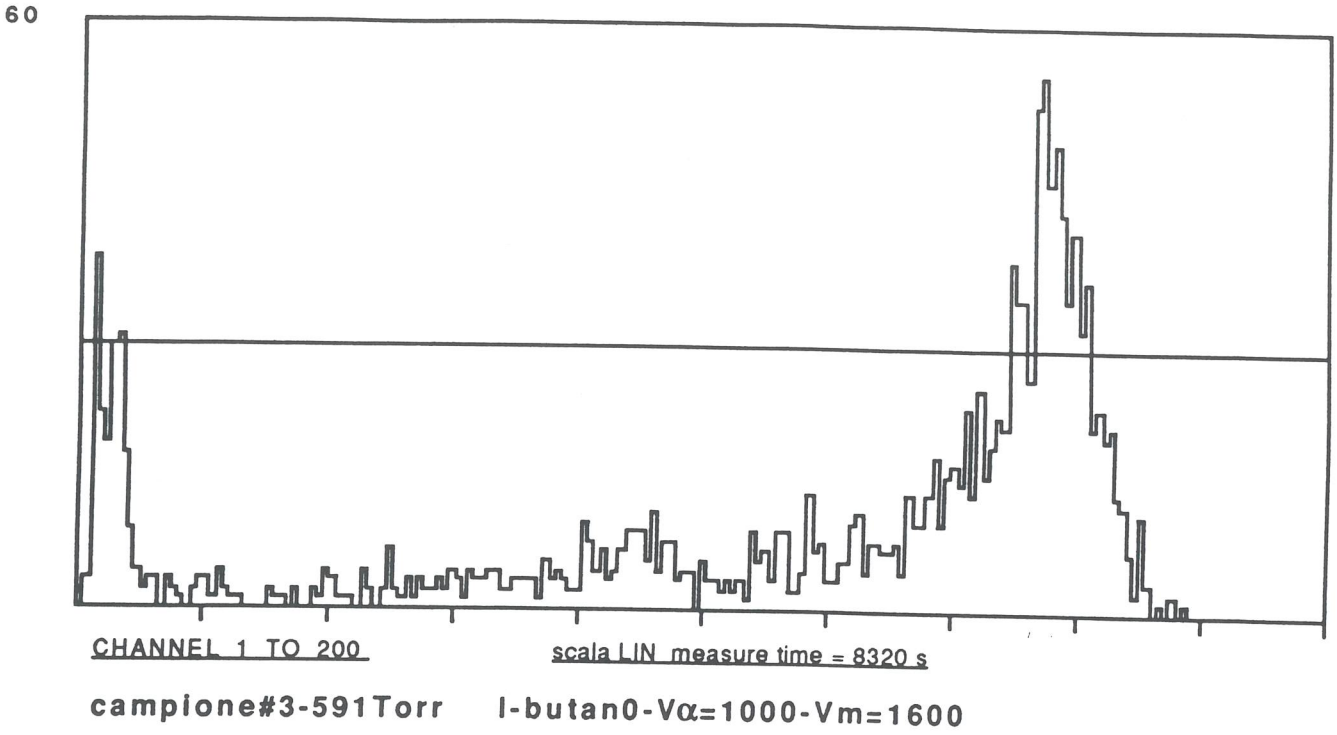
60
CHANNEL 1 TO 200
scala LIN measure time = 8320 s
campione#3-591Torr
l-butan0-Vα=1000-Vm=1600

Fig. 18

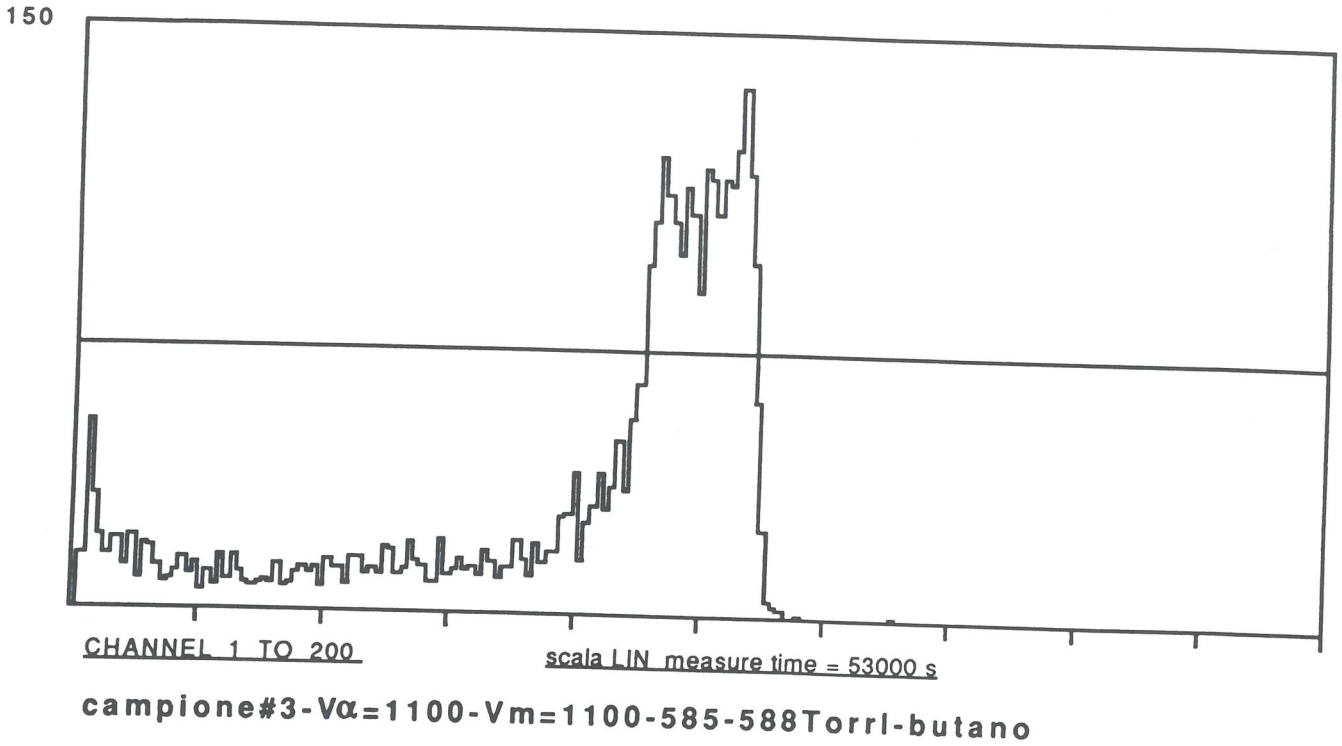
150
CHANNEL 1 TO 200
scala LIN measure time = 53000 s
campione#3-Vα=1100-Vm=1100-585-588Torrl-butano

Fig. 19

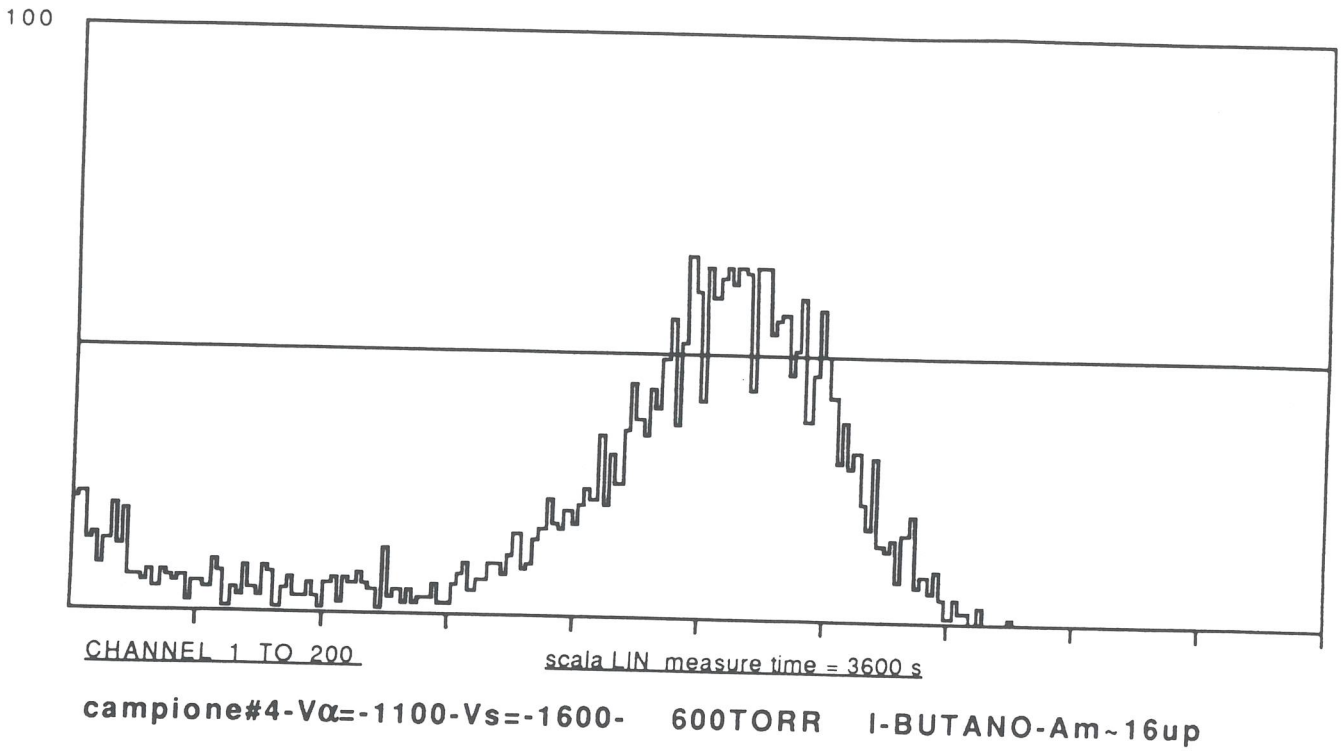
100
CHANNEL 1 TO 200
scala LIN measure time = 3600 s
campione#4-Vα=-1100-Vs=-1600- 600TORR I-BUTANO-Am~16up

Fig. 20

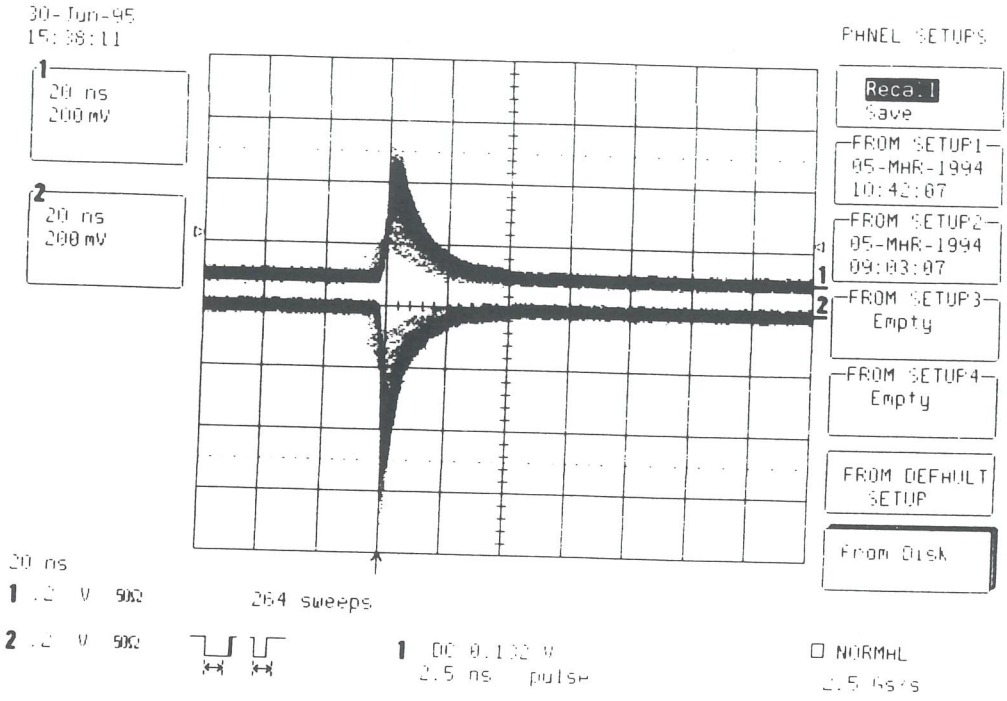
30-Jun-95
15:38:11
1
20 ns
200 mV
2
20 ns
200 mV
PANEL SETUPS
Recall
Save
FROM SETUP1
05-MAR-1994
10:42:07
FROM SETUP2
05-MAR-1994
09:03:07
FROM SETUP3
Empty
FROM SETUP4
Empty
FROM DEFAULT
SETUP
From Disk
20 ns
264 sweeps
NORMAL

Fig. 21

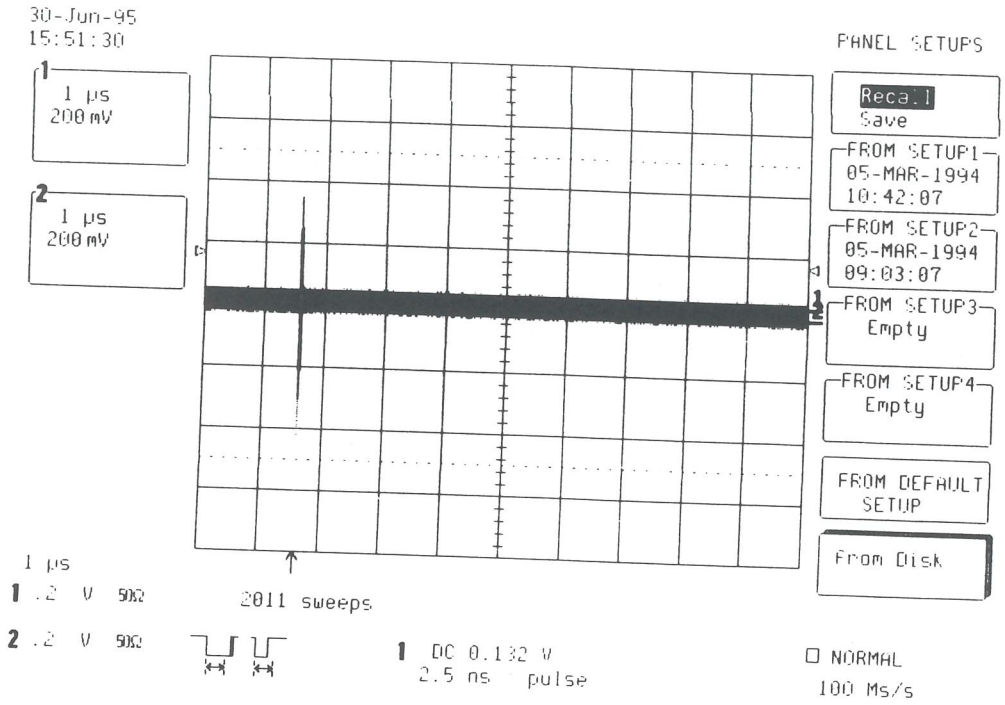
30-Jun-95
15:51:30
1 µs
200 mV
2 1 µs
200 mV
PANEL SETUPS
Recall
Save
FROM SETUP1
05-MAR-1994
10:42:07
FROM SETUP2
05-MAR-1994
09:03:07
FROM SETUP3
Empty
FROM SETUP4
Empty
FROM DEFAULT
SETUP
From Disk
1 µs
1 .2 V 50Ω
2 .2 V 50Ω
2011 sweeps
1 DC 0.132 V
2.5 ns pulse
NORMAL
100 Ms/s

Fig. 22

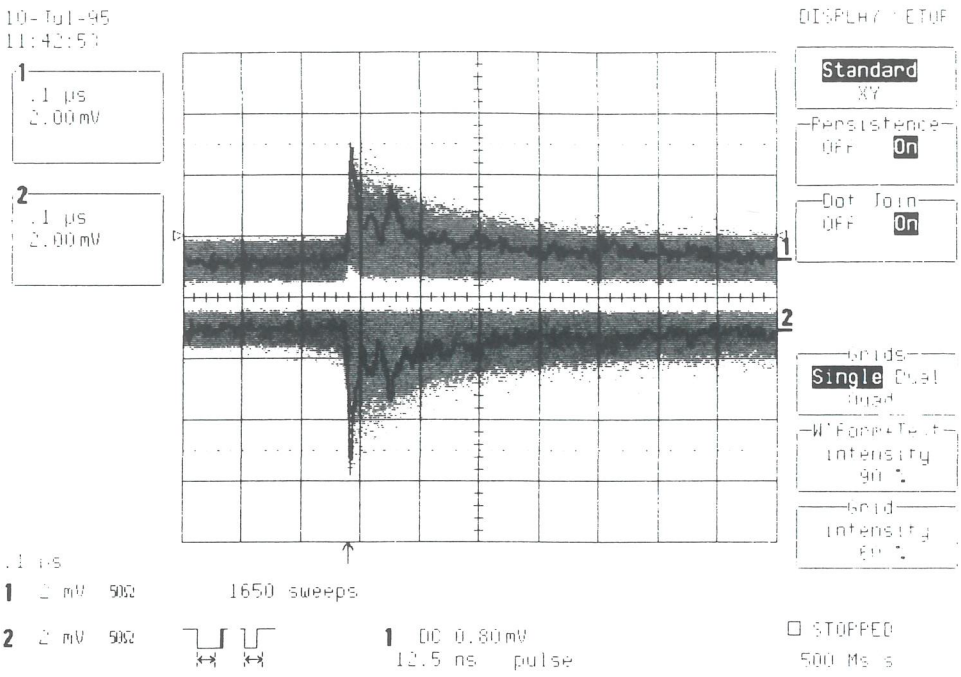
10-Jul-95
11:42:57
1
.1 µs
2.00mV
2
.1 µs
2.00mV
Standard
XY
Persistence
OFF
On
Dot Join
OFF
On
Single
Intensity
90 %
Intensity
1650 sweeps
1 DC 0.80mV
12.5 ns pulse
STOPPED
500 Ms/s

Fig. 23

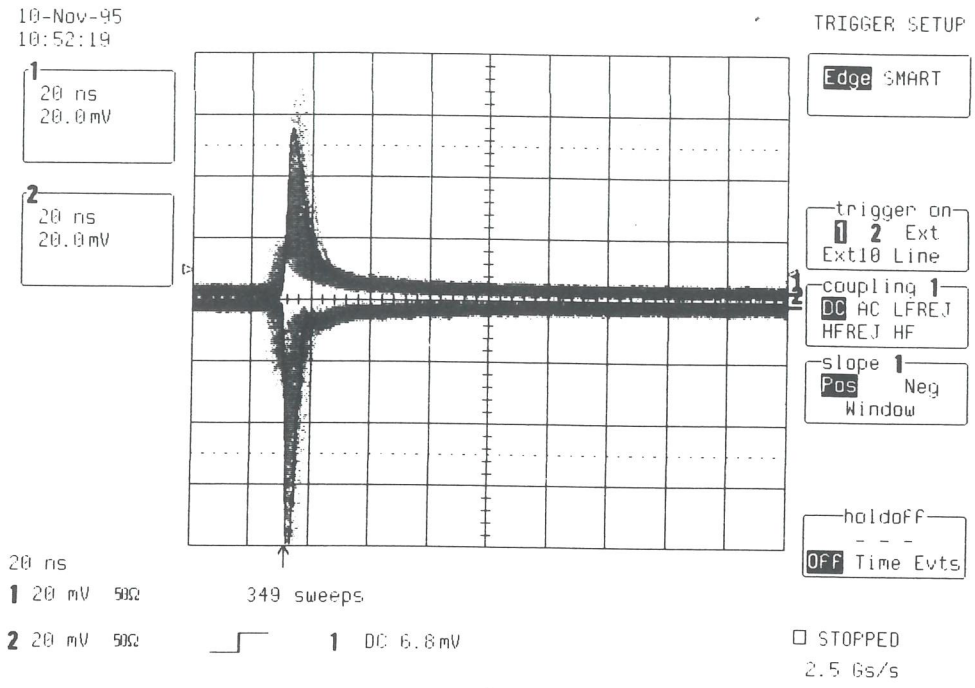
10-Nov-95
10:52:19
1
20 ns
20.0mV
2
20 ns
20.0mV
TRIGGER SETUP
Edge SMART
trigger on
1 2 Ext
Ext10 Line
coupling 1
DC AC LFREJ
HFREJ HF
slope 1
Pos Neg
Window
holdoff
Off Time Evts
20 ns
1 20 mV 50Ω
2 20 mV 50Ω
349 sweeps
1 DC 6.8mV
STOPPED
2.5 Gs/s

Fig. 24

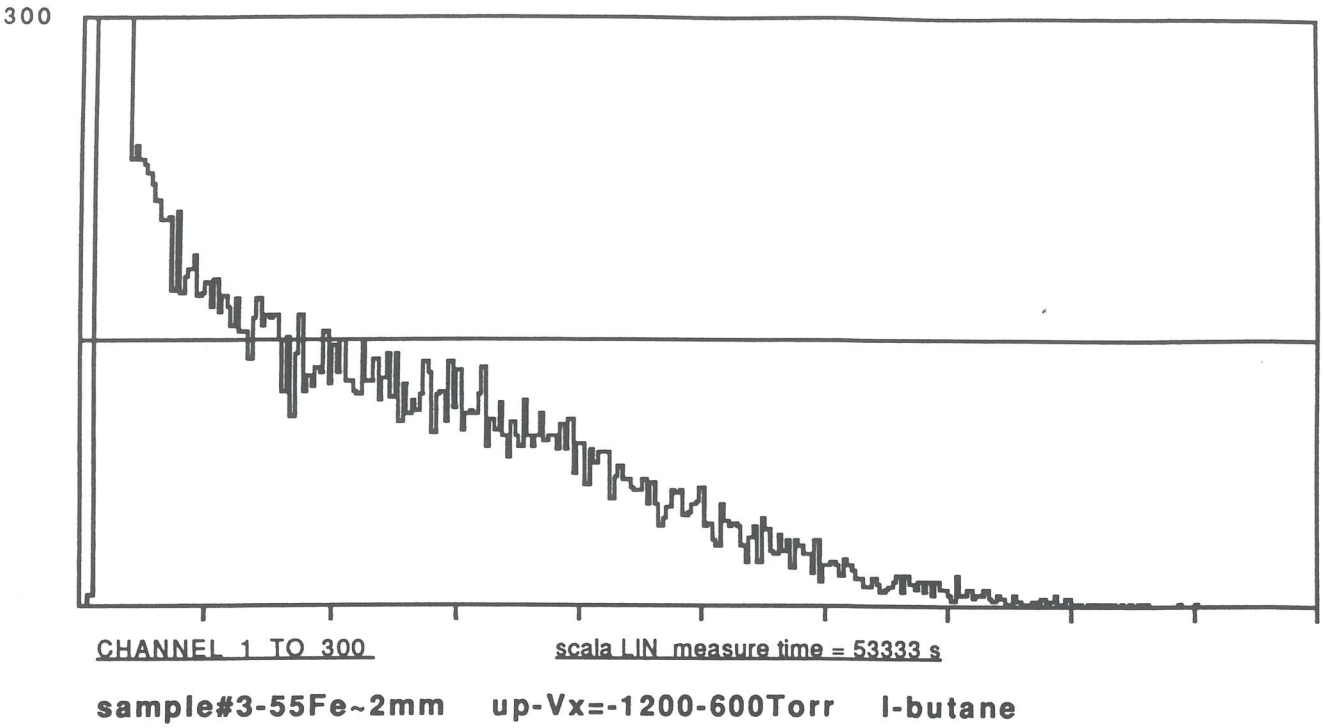
300
CHANNEL 1 TO 300
scala LIN measure time = 53333 s
sample#3-55Fe~2mm up-Vx=-1200-600Torr l-butane

Fig. 25

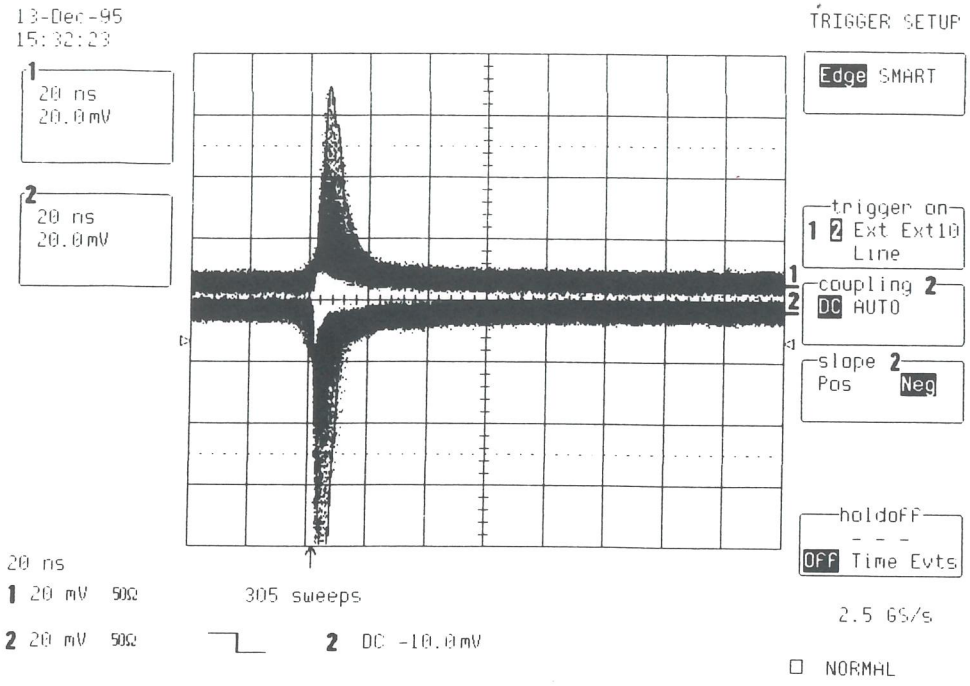
13-Dec-95
15:32:23
1
20 ns
20.0mV
2
20 ns
20.0mV
TRIGGER SETUP
Edge SMART
trigger on
1 2 Ext Ext10
Line
coupling 2
DC AUTO
slope 2
Pos Neg
holdoff
- - -
Off Time Evts
20 ns
1 20 mV 50Ω
2 20 mV 50Ω
305 sweeps
2 DC -10.0mV
2.5 GS/s
NORMAL

Fig. 26

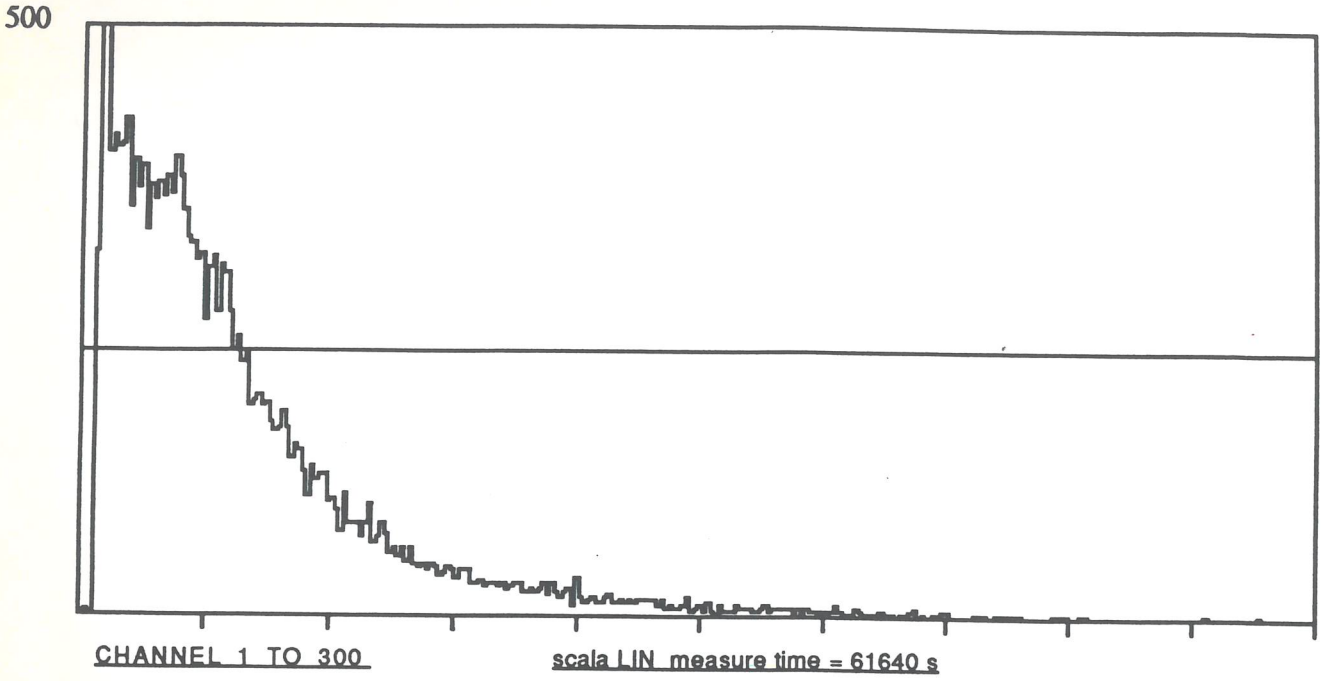
500
CHANNEL 1 TO 300
scala LIN measure time = 61640 s
Sample#3-Vb=-1200V-600Torr-Isobut.14C~2mm.UP

Fig. 27